

Spring 5-31-1986

Deconvolution techniques with applications in cardiovascular systems analysis

Lakshminarayan Rajaram
New Jersey Institute of Technology

Follow this and additional works at: <https://digitalcommons.njit.edu/theses>



Part of the [Applied Mathematics Commons](#)

Recommended Citation

Rajaram, Lakshminarayan, "Deconvolution techniques with applications in cardiovascular systems analysis" (1986). *Theses*. 1440.

<https://digitalcommons.njit.edu/theses/1440>

This Thesis is brought to you for free and open access by the Electronic Theses and Dissertations at Digital Commons @ NJIT. It has been accepted for inclusion in Theses by an authorized administrator of Digital Commons @ NJIT. For more information, please contact digitalcommons@njit.edu.

Copyright Warning & Restrictions

The copyright law of the United States (Title 17, United States Code) governs the making of photocopies or other reproductions of copyrighted material.

Under certain conditions specified in the law, libraries and archives are authorized to furnish a photocopy or other reproduction. One of these specified conditions is that the photocopy or reproduction is not to be “used for any purpose other than private study, scholarship, or research.” If a user makes a request for, or later uses, a photocopy or reproduction for purposes in excess of “fair use” that user may be liable for copyright infringement,

This institution reserves the right to refuse to accept a copying order if, in its judgment, fulfillment of the order would involve violation of copyright law.

Please Note: The author retains the copyright while the New Jersey Institute of Technology reserves the right to distribute this thesis or dissertation

Printing note: If you do not wish to print this page, then select “Pages from: first page # to: last page #” on the print dialog screen

The Van Houten library has removed some of the personal information and all signatures from the approval page and biographical sketches of theses and dissertations in order to protect the identity of NJIT graduates and faculty.

DECONVOLUTION TECHNIQUES WITH APPLICATIONS
IN CARDIOVASCULAR SYSTEMS ANALYSIS

by

Lakshminarayan Rajaram

Thesis submitted to the Faculty of the Graduate School
of New Jersey Institute of Technology in partial
fulfillment of the requirements for the degree of
Master of Science
1986

APPROVAL SHEET

Title of Thesis: Deconvolution techniques with applications
in cardiovascular systems analysis

Name of Candidate: Lakshminarayan Rajaram
Master of Science, 1986

Thesis and Abstract approved:

Dr. Denis Blackmore Professor Department of Mathematics New Jersey Institute of Technology	Date
---	------

Dr. Swamy Laxminarayan Department of Biomedical Engg. U. of Medicine & Dentistry of N.J.	Date
--	------

Dr. Roy Plastock Department of Mathematics New Jersey Institute of Technology	Date
---	------

VITA

Name: Lakshminarayan Rajaram.

Permanent address:

Degree and date to be conferred: M.S., May 1986

Date of birth:

Place of birth:

Secondary education: Siddaganga High School, May 1969.

<u>Collegiate institutions</u> <u>attended</u>	<u>Dates</u>	<u>Degree</u>	<u>Date of degree</u>
Government Science College Tumkur, Karnataka State India	1972-75	B.Sc.	July 1975
Mangalagangothri Mangalore, Karnataka State India	1975-77	M.Sc.	July 1977
New Jersey Institute of Technology Newark, N.J.	1983-86	M.S.	May 1986

Major : Applied Mathematics

Publications:

- . Spectral Analysis applications in the characterization of sleep-wake patterns of normal and near-miss infants for the Sudden Infant Death Syndrome.
- . Estimation of Impulse Response Function by deconvolution technique in the characterization of physiological system.

Positions held:

- . February 1981 - December 1982, Lecturer in Mathematics, NMKRV College for Women, Bangalore, India.
- . September 1984 - May 1986, Teaching Assistant, Department of Mathematics, New Jersey Institute of Technology, Newark, New Jersey.

ABSTRACT

Title of Thesis: Deconvolution Techniques with applications
in Cardiovascular systems analysis

Lakshminarayan Rajaram, Master of Science, 1986

Thesis directed by: Dr. D. Blackmore, Professor of Mathematics

System characterization by means of Impulse and Frequency Response Functions are well known in classical linear systems analysis. Impulse Response Function is a time domain description of a linear system whereas the Frequency Response Function represents the frequency domain counterpart. Linear systems are often characterized in frequency domain. In many biological research applications, it becomes necessary to examine the impulse response function in order to understand the behavior of the system under investigation. One such application is the arterial system in cardiovascular dynamics. It has been shown that although both representations are identical, some aspects of the arterial system are better emphasized by one description than by the other. In order to obtain accurate estimates of the impulse response function it is desirable to solve the convolution integral in the time domain by deconvolving the system input and output time histories. Solution of the convolution integral is however extremely complex and requires the use of numerical approximation methods.

This work is primarily focused on developing these numerical approximation procedures with particular application emphasis on the arterial system.

Blank Page

ACKNOWLEDGEMENTS

This project was done in collaboration with the Department of Biomedical Engineering and Laboratory Computer Center of the University of Medicine and Dentistry of New Jersey, Newark. The author would like to express his gratitude to Dr. Les Michelson of UMDNJ for providing the computer support for carrying out the project and to Drs. Denis Blackmore and Swamy Laxminarayan for the constant help, encouragement and guidance they offered throughout the Project period.

TABLE OF CONTENTS

ACKNOWLEDGMENT	iv
I. INTRODUCTION	1
1. Arterial System	1
II. MATHEMATICAL BASIS	4
1. Input Impedance of the Arterial System	4
2. Arterial Models	4
3. Impulse Response Function	6
III. METHODS	10
1. Convolution Integral	10
2. Direct Numerical Method	10
3. Cramer's Rule	13
4. Method of Gaussian Elimination	13
5. Iterative Methods	13
6. Modified Method	20
IV. RESULTS AND DISCUSSIONS	30
1. RC Filter Network	30
2. Windkessel Model	37
V. REFERENCES	41
VI. FIGURES	42

1. INTRODUCTION

System characterization by means of Impulse and Frequency Response functions are well known in classical linear systems analysis. Impulse response function is a time domain description of a linear system whereas the Frequency Response Function represents its frequency domain counterpart. Linear systems are often characterized in frequency domain. In many biological research applications, it becomes necessary to examine the impulse response function in order to understand the behavior of the system under investigation. One such application is the arterial system in cardiovascular dynamics. It has been shown that although both representations are identical, some aspects of the arterial system are better emphasized by one description than by the other (Laxminarayan et al, 1978). In order to obtain accurate estimates of the impulse response function it is desirable to solve the convolution integral in the time domain by deconvolving the system input and output time histories. Solution of the convolution integral is however extremely complex and requires the use of numerical approximation methods. This work is primarily focused on developing these numerical approximation procedures with particular application emphasis on the arterial system.

1.1. ARTERIAL SYSTEM

The functioning of the arterial system in cardiovascular physiology is to transport blood ejected from the left

ventricular to the peripheries. The arterial system consists of a complex branched network of tubes varying in size from very large to tiny arteries. The large artery, the aorta, acts as a "compression chamber" storing by its capacitance the stroke volume for delivery at a constant rate to the peripheries. As in any hydraulic system the dynamics of the arterial tree can be characterized by measuring the pressure and flow of blood in the system. It is widely known that the pressure and flow measurements made in the aorta can be used to characterize the entire arterial system (Bergel, 1972).

In the past, systems engineering methods have been applied to the measured pressure and flow data for characterizing the arterial system. Utilizing these methods, the dynamics of any given system can be described either in the time domain or in the frequency domain provided the system is assumed to be linear. The frequency domain method involves computing an input-output relationship in terms of the frequency response function or the so-called input impedance function for the arterial system (Westerhof et al, 1980). The time domain counterpart is given by the impulse response function of the system (Laxminarayan et al, 1980).

The input-impedance of the arterial system has been widely studied in recent years and the arterial impulse response function has been studied by Laxminarayan et al.. Both of these descriptions contain identical information excepting that some system properties are emphasized better by one than the other. As in any electrical analog, a system can be

described by a resistance, compliance and an inductance term. In terms of these elements, input-impedance of the arterial system emphasizes the peripheral resistance, whereas in the impulse response function, the emphasis is on the total arterial compliance. Another important aspect of arterial dynamics is the reflection phenomenon of the pressure and flow waves in the system (Van Den & Bos et al 1976 and Laxminarayan et al 1979a). Recent studies have shown that the arterial reflection can be better studied by means of the impulse response function than the arterial input impedance (Laxminarayan et al, 1978). This is one of the major reasons why it is preferable to use the impulse response function approach for studying arterial reflections. However the methods for computing the impulse response function of the arterial system have several complexities which are discussed in the next section.

The aim of the project is to investigate the computational methods for estimating the impulse response function with application emphasis on the arterial system. The methods developed are tested using relevant analytical models and a model of the arterial system.

2. MATHEMATICAL BASIS

2.1 Input-Impedance of the Arterial System

Assuming the arterial system to be linear, the input-impedance of the system is estimated by applying linear system analysis concepts. The linearity of the arterial system has been established by several investigators in the past (Westerhof et al, 1979). If $p(t)$ and $f(t)$ are respectively the pressure drop and flow through the system, the system function can be described by means of the convolution integral given by:

$$p(t) = \int_0^t f(t-u) \cdot z(u) \, du \dots\dots\dots (2.1.1)$$

where $z(t)$ is the impulse response function.

Expressing this convolution as a product in the frequency domain, we can write

$$P(jw) = F(jw) \cdot Z(jw) \dots\dots\dots (2.1.1a)$$

where P, F, Z are the Fourier transforms of $p(t), f(t), z(t)$ respectively, w is the angular frequency and $j = \text{SQRT}(-1)$.

Hence,

$$Z(jw) = P(jw)/F(jw) \dots\dots\dots (2.1.2)$$

In other words, the input-impedance of the arterial system, $Z(jw)$, is calculated by dividing the moduli of pressure and flow harmonics and subtracting the corresponding phases. This method has been commonly used to compute $Z(jw)$ (Westerhof et al 1979 and Laxminarayan et al 1979b).

2.2 ARTERIAL MODELS

In the past, two specific models of the arterial system have

been commonly used to understand the behavior or dynamics of the arterial system (Laxminarayan et al 1978). These models are:

1. A Windkessel Model
2. Uniform Tube Model

A Windkessel model is an electrical analog of the arterial system under normal conditions. The electrical circuit for this is given in Figure A.1, where L =inductance, R_C ; R_p are two resistors and C =capacitor. Using this model, we can simulate the functions of the arterial system under normal conditions.

A second model which imitates the arterial system under abnormal conditions (i.e. when occlusions are present in the arterial system) is the Uniform Elastic Tube model. This model is given in the Figure A.2. Due to the presence of occlusion at the end of the tube, the pressure and flow waves entering the tube are reflected back at the end. In other words this model enables us to study the arterial reflection phenomenon (Laxminarayan et al 1978).

2.2(a) Input-impedance of the Windkessel model

The input-impedance of the Windkessel model of figure A.1 is given by (Westerhof et al 1979).

$$Z(j\omega) = R_p + j\omega L + (1/C) (1/(j\omega + 1/\tau)) \dots \dots \dots (2.2.1)$$

where $\tau = R_p \cdot C$, $\omega = 2\pi f$ ($\pi = 22/7$), f = frequency in HZ.

$Z(j\omega)$ is a complex quantity and has both a modulus and phase.

The typical characteristics of input-impedance of the Windkessel model are:

1. Input-impedance at zero HZ is always equal to R_p which is the peripheral resistance (= mean pressure/mean flow).
2. At higher frequencies, the input-impedance approximates R_c which is the characteristics impedance of the aorta.
3. The total arterial compliance, C , of the arterial system can be calculated from:

$$\tau = R_p C \quad \text{i.e. } C = (\tau/R_p)$$

where τ is estimated independently by fitting an exponential to the diastolic part of the arterial pressure waveform.

2.3 Impulse Response Function:

In practice, the impulse response function of the Windkessel model of figure A.1 is given by:

$$z(t) = R_c \cdot \delta(t) + L \cdot \delta'(t) + (1/C) (\exp(-t/\tau)) \dots (2.3.1)$$

where $\delta(t)$ is the Dirac delta function and $\delta'(t)$, the time derivative of the delta function (doublet).

For a periodic excitation of the model with a period T , we find:

$$z(t) = R_c \cdot \delta(t) + L \cdot \delta'(t) + \frac{\exp(-t/\tau)}{C(1-\exp(-T/\tau))} \dots (2.3.2)$$

The theoretical impulse response function of the four element Windkessel model is composed of a delta function plus a doublet and an exponentially decaying function with time constant τ . The height of the exponential decay, extrapolated to time zero, gives (using τ & T) the Total

Arterial Compliance (Laxminarayan et al 1978).

The impulse response function of the arterial system can be visualized as the response in terms of pressure when a unit impulse of flow is delivered to the system. The impulse response function can be calculated either directly by using equation(2.1.1) i.e. by deconvolving pressure and flow time histories or indirectly by inverse Fourier transforming the input-impedance, $Z(j\omega)$, that is

$$z(t) = \int_0^{\infty} Z(j\omega) \cdot \exp(j\omega t) d\omega \dots\dots\dots(2.3.3)$$

The indirect method of computing the impulse response function of the arterial system by inverse Fourier transforming $Z(j\omega)$ is investigated by Laxminarayan et al. (1978).

The indirect method as identified in equation (2.3.3) suffers from one major flaw. The upper limit of integration in equation(2.3.3) for performing the inverse transformation indicates that we need to have a knowledge of $Z(j\omega)$ at an infinite set of frequencies. In practice however we cannot satisfy this condition since it is not possible to compute $Z(j\omega)$ for frequencies above 40HZ. This is because above this frequency range, noise in the data makes it meaningless to compute $Z(j\omega)$. Therefore the input-impedance has to be truncated at some finite frequency prior to inverse Fourier transformation. If the values of $Z(j\omega)$ have reached steady zero values at the cut-off frequency, then the inverse Fourier transformation yields

meaningful results. Unfortunately this is not the case for the arterial system. In fact, it is well established that the input-impedance at higher frequencies stays constant and is equal to the characteristic impedance of the aorta. Therefore truncation of the input-impedance at some finite frequency implies the presence of a mathematical window. The effects of this window appear as oscillations superimposed on the true impulse response function. Therefore in order to eliminate these undesired components from the impulse response function, some form of frequency domain smoothing has to be applied before inverse transforming $Z(j\omega)$. Such smoothing procedures have been shown to yield meaningful estimates of the impulse response function (Laxminarayan et al., 1978).

While this method seems to provide a reasonable solution under control conditions, the solution may not be adequate when reflections are present in the arterial system. Theoretically, reflections in the arterial system should show up as distinct peaks in the impulse response function. When frequency domain smoothing is applied, there is a strong likelihood of missing this important information. This is especially the case when the amplitudes of these reflection peaks are relatively small compared to the initial delta function one obtains in the impulse response function. Under these conditions, therefore it is much better to compute the impulse response function without applying any form of smoothing. This implies that we need to

apply direct techniques i.e. deconvolution using equation (2.1.1), to estimate the impulse response function.

The procedure for computing the impulse response function by the direct method involves finding an acceptable solution to the convolution integral. In the following section, different methods are presented and their relative advantages and disadvantages are discussed.

3. METHODS

3.1 CONVOLUTION INTEGRAL:

The convolution integral is given by (Bendat & Piersol, 1972)

$$p(t) = \int_{-\infty}^{\infty} f(t-\tau) \cdot z(\tau) d\tau \quad \text{----- (3.1)}$$

For the case of the arterial system where $p(t)$ = Pressure drop over the arterial system, $f(t)$ = Flow through the arterial system and $z(t)$ is the impulse response function.

In order to compute the arterial impulse response function, we need to apply the deconvolution procedure to the pressure and flow data. Knowing $f(t)$ and $p(t)$, we would like to calculate $z(t)$.

3.2 DIRECT NUMERICAL METHOD:

The direct numerical method resolves in to expressing equations as a summation.

$$p_i = \sum_{l=0}^{i-1} f_{i-l} z_l \Delta t \quad \text{for } i = 0, 1, 2, \dots, n.$$

i.e. we have a system of equations:

$$p_0 = f_0 z_0 \Delta t$$

$$p_1 = [f_1 z_0 + f_0 z_1] \Delta t$$

$$p_2 = [f_2 z_0 + f_1 z_1 + f_0 z_2] \Delta t \quad \text{----- (3.2.1)}$$

.

.

.

$$p_n = [f_n z_0 + f_{n-1} z_1 + \dots + f_0 z_n] \Delta t$$

So we have a set of simultaneous equations in z for which we seek the solution. In matrix notation, we write the set of equations as: $P = F Z \Delta t$

$$\begin{bmatrix} p_0 \\ p_1 \\ p_2 \\ \cdot \\ \cdot \\ \cdot \\ p_n \end{bmatrix} = \begin{bmatrix} f_0 & 0 & 0 & \cdot & \cdot & 0 \\ f_1 & f_0 & 0 & \cdot & \cdot & 0 \\ f_2 & f_1 & f_0 & \cdot & \cdot & 0 \\ \cdot & \cdot & \cdot & \cdot & \cdot & \cdot \\ \cdot & \cdot & \cdot & \cdot & \cdot & \cdot \\ \cdot & \cdot & \cdot & \cdot & \cdot & \cdot \\ f_n & f_{n-1} & f_{n-2} & \cdot & \cdot & f_0 \end{bmatrix} \begin{bmatrix} z_0 \\ z_1 \\ z_2 \\ \cdot \\ \cdot \\ \cdot \\ z_n \end{bmatrix} \Delta t$$

Now if we introduce additional subscripts, we obtain:

$$\begin{bmatrix} p_0 \\ p_1 \\ p_2 \\ \cdot \\ \cdot \\ \cdot \\ p_n \end{bmatrix} = \begin{bmatrix} f_{00} & 0 & 0 & \cdot & \cdot & 0 \\ f_{10} & f_{11} & 0 & \cdot & \cdot & 0 \\ f_{20} & f_{21} & f_{22} & \cdot & \cdot & 0 \\ \cdot & \cdot & \cdot & \cdot & \cdot & \cdot \\ \cdot & \cdot & \cdot & \cdot & \cdot & \cdot \\ \cdot & \cdot & \cdot & \cdot & \cdot & \cdot \\ f_{n0} & f_{n1} & f_{n2} & \cdot & \cdot & f_{nn} \end{bmatrix} \begin{bmatrix} z_0 \\ z_1 \\ z_2 \\ \cdot \\ \cdot \\ \cdot \\ z_n \end{bmatrix} \Delta t$$

i.e.

$$\begin{aligned}
 p_0 &= f_{00} z_0 \Delta t \\
 p_1 &= [f_{10} z_0 + f_{11} z_1] \Delta t \\
 p_2 &= [f_{20} z_0 + f_{21} z_1 + f_{22} z_2] \Delta t \\
 &\vdots \\
 &\text{----- (3.2.2)} \\
 p_n &= [f_{n0} z_0 + f_{n1} z_1 + \cdot \cdot + f_{nn} z_n] \Delta t
 \end{aligned}$$

Note that (3.2.1) and (3.2.2) are exactly the same excepting for the transformation in the matrix element notation.

But $f_0 = f_{00} = f_{11} = f_{22} = \cdot \cdot \cdot = f_{nn}$.

$$\begin{aligned}
 f_1 &= f_{10} = f_{21} = f_{32} = \dots \\
 f_2 &= f_{20} = f_{31} = f_{42} = \dots \\
 f_3 &= f_{30} = f_{41} = f_{52} = \dots \\
 &\cdot \quad \quad \cdot \quad \quad \cdot \quad \quad \cdot \\
 &\cdot \quad \quad \cdot \quad \quad \cdot \quad \quad \cdot \\
 &\cdot \quad \quad \cdot \quad \quad \cdot \quad \quad \cdot
 \end{aligned}$$

From equation (3.2.2), we write the following set of equations for deconvolution.

$$\begin{aligned}
 z_0 &= (1/f_{00} \Delta t) p_0 \\
 z_1 &= 1/f_{11} ((p_1/\Delta t) - f_{10} z_0) \\
 z_2 &= 1/f_{22} ((p_2/\Delta t) - (f_{20} z_0 + f_{21} z_1)) \\
 &\cdot \quad \quad \cdot \quad \quad \cdot \quad \quad \cdot \\
 &\cdot \quad \quad \cdot \quad \quad \cdot \quad \quad \cdot \\
 z_n &= 1/f_{nn} ((p_n/\Delta t) - (f_{n0} z_0 + f_{n1} z_1 + \dots + f_{n,n-1} z_{n-1}))
 \end{aligned}$$

Or in general terms,

$$\begin{aligned}
 z_i &= (1/f_{ii}) ((p_i/\Delta t) - \sum_{k=0}^{i-1} f_{ik} z_k) \\
 &\text{for } i = 0, 1, 2, 3, \dots, n.
 \end{aligned}
 \quad \text{----- (3.2.3)}$$

Effectively, we are seeking a solution for:

$$F Z \Delta t = P$$

Since $p \neq 0$ (not necessarily), the system of equations are non-homogeneous. A system of non-homogeneous equations in 'n' unknowns has a unique solution provided that the rank of its co-efficient matrix F is 'n', i.e. $|F| \neq 0$

3.3 CRAMER'S RULE:

One method of solving a system of 'n' non-homogeneous equations is by means of determinants using Cramer's rule.

i.e. if the determinant of a system $|F| \neq 0$, then the system

$F Z = P$ has the unique solution, namely:

$$z_i = |F_i| / |F|$$

where F_i is the matrix obtained from F , by replacing its i th column with the column of constants i.e. p 's.

If the determinant of the co-efficients is small as compared to the co-efficients themselves, then small changes in the co-efficients can be expected to lead to very large changes in the solution, implying that these equations are ill-conditioned.

3.4 METHOD OF GAUSSIAN ELIMINATION:

Another method of solution is by inverting the square matrix F in $F Z = P$.

$$\text{i.e. } Z = F^{-1} P$$

This can be achieved by the method of Gaussian elimination with pivoting. However, this gives rise to unacceptable results since such a technique does not exploit the presence of zeros, where as in the convolution problem we will be dealing with matrices some of whose elements are zeros. Therefore it is prudent to examine some of the iterative methods that are available.

3.5 ITERATIVE METHODS:

In the iterative methods for solving, $F Z = P$, the solution is obtained by splitting the matrix F in

to two parts, namely,

$$F = (M - N)$$

To solve $F \Delta t Z = P$, we define a sequence of vectors $z^{(k)}$ by the equations:

$$M z^{(k+1)} = N z^{(k)} + P / \Delta t \quad k = 0, 1, 2, \dots$$

where z must be specified.

Three examples of splitting F are worth discussing.

3.5.1 POINT-JACOBI METHOD:

This method is also called 'The method of simultaneous displacements'. Here we let D be the diagonal matrix whose main diagonal agrees with the main diagonal of the matrix F .

i.e. $D =$

$$\begin{bmatrix} f_{00} & 0 & 0 & 0 & \cdot & \cdot & \cdot & 0 \\ 0 & f_{11} & 0 & 0 & 0 & \cdot & \cdot & 0 \\ 0 & 0 & f_{22} & 0 & 0 & \cdot & \cdot & 0 \\ \cdot & \cdot & \cdot & \cdot & \cdot & \cdot & \cdot & \cdot \\ \cdot & \cdot & \cdot & \cdot & \cdot & \cdot & \cdot & \cdot \\ \cdot & \cdot & \cdot & \cdot & \cdot & \cdot & \cdot & \cdot \\ 0 & 0 & 0 & 0 & 0 & \cdot & \cdot & f_{nn} \end{bmatrix}$$

where

$$F = \begin{bmatrix} f_{00} & f_{01} & f_{02} & f_{03} & \cdot & \cdot & \cdot & f_{0n} \\ f_{10} & f_{11} & f_{12} & f_{13} & \cdot & \cdot & \cdot & f_{1n} \\ \cdot & \cdot & \cdot & \cdot & \cdot & \cdot & \cdot & \cdot \\ \cdot & \cdot & \cdot & \cdot & \cdot & \cdot & \cdot & \cdot \\ f_{n0} & f_{n1} & f_{n2} & f_{n3} & \cdot & \cdot & \cdot & f_{nn} \end{bmatrix}$$

Suppose we let $M = D$ and $N = D - F$ ($F = M - N$)

$$M = \begin{bmatrix} f_{00} & 0 & 0 & 0 & 0 & \cdot & \cdot & \cdot & 0 \\ 0 & f_{11} & 0 & 0 & 0 & \cdot & \cdot & \cdot & 0 \\ 0 & 0 & f_{22} & 0 & 0 & \cdot & \cdot & \cdot & 0 \\ 0 & 0 & 0 & f_{33} & 0 & \cdot & \cdot & \cdot & 0 \\ \cdot & \cdot & \cdot & \cdot & \cdot & \cdot & \cdot & \cdot & 0 \\ \cdot & \cdot & \cdot & \cdot & \cdot & \cdot & \cdot & \cdot & 0 \\ 0 & 0 & 0 & 0 & 0 & 0 & 0 & 0 & f_{nn} \end{bmatrix}$$

Since $N = D - F$, we have,

$$N = \begin{bmatrix} 0 & -f_{01} & -f_{02} & -f_{03} & \cdot & \cdot & \cdot & -f_{0n} \\ -f_{10} & 0 & -f_{12} & -f_{13} & \cdot & \cdot & \cdot & -f_{1n} \\ -f_{20} & -f_{21} & 0 & -f_{23} & \cdot & \cdot & \cdot & -f_{2n} \\ \cdot & \cdot & \cdot & \cdot & \cdot & \cdot & \cdot & \cdot \\ \cdot & \cdot & \cdot & \cdot & \cdot & \cdot & \cdot & \cdot \\ \cdot & \cdot & \cdot & \cdot & \cdot & \cdot & \cdot & \cdot \\ -f_{n0} & -f_{n1} & -f_{n2} & -f_{n3} & \cdot & \cdot & \cdot & 0 \end{bmatrix}$$

Substituting these in:

$$M z^{(k+1)} = N z^{(k)} + p/\Delta t, \text{ we get}$$

$$\begin{bmatrix} f_{00} & 0 & 0 & \cdot & \cdot & 0 \\ 0 & f_{11} & 0 & \cdot & \cdot & 0 \\ 0 & 0 & f_{22} & \cdot & \cdot & 0 \\ \cdot & \cdot & \cdot & \cdot & \cdot & \cdot \\ \cdot & \cdot & \cdot & \cdot & \cdot & \cdot \\ 0 & 0 & 0 & 0 & 0 & f_{nn} \end{bmatrix} \begin{bmatrix} z_0 \\ z_1 \\ z_2 \\ \cdot \\ \cdot \\ z_n \end{bmatrix}^{(k+1)} =$$

$$\begin{bmatrix} 0 & -f_{01} & -f_{02} & \cdot & \cdot & -f_{0n} \\ -f_{10} & 0 & -f_{12} & \cdot & \cdot & -f_{1n} \\ -f_{20} & -f_{21} & 0 & \cdot & \cdot & -f_{2n} \\ \cdot & \cdot & \cdot & \cdot & \cdot & \cdot \\ \cdot & \cdot & \cdot & \cdot & \cdot & \cdot \\ \cdot & \cdot & \cdot & \cdot & \cdot & \cdot \\ -f_{n0} & -f_{n1} & -f_{n2} & \cdot & \cdot & 0 \end{bmatrix} \begin{bmatrix} z_0 \\ z_1 \\ z_2 \\ \cdot \\ \cdot \\ \cdot \\ z_n \end{bmatrix}^{(k)} + \begin{bmatrix} p_0 \\ p_1 \\ p_2 \\ \cdot \\ \cdot \\ \cdot \\ p_n \end{bmatrix} (1/\Delta t)$$

Expanding and simplifying we get,

$$1. f_{00} z_0^{(k+1)} + f_{01} z_1^{(k)} + \dots + f_{0n} z_n^{(k)} = p_0/\Delta t$$

$$2. f_{11} z_1^{(k+1)} + f_{10} z_0^{(k)} + \dots + f_{1n} z_n^{(k)} = p_1/\Delta t$$

$$\begin{array}{cccccccc}
 \cdot & \cdot & \cdot & \cdot & \cdot & \cdot & \cdot & \cdot \\
 \cdot & \cdot & \cdot & \cdot & \cdot & \cdot & \cdot & \cdot \\
 \cdot & \cdot & \cdot & \cdot & \cdot & \cdot & \cdot & \cdot
 \end{array}$$

$$f_{n0} z_0^{(k)} + f_{n1} z_1^{(k)} + \dots + f_{nn} z_n^{(k+1)} = p_n/\Delta t.$$

Take for e.g. (1) above:

$$f_{00} z_0^{(k+1)} + f_{00} z_0^{(k)} + f_{01} z_1^{(k)} + \dots -$$

$$+ f_{0n} z_n^{(k)} = p_0/\Delta t + f_{00} z_0^{(k)}$$

$$\text{i.e. } f_{00} z_0^{(k+1)} = f_{00} z_0^{(k)} + p_0/\Delta t - \sum_{l=1}^n f_{0l} z_l^{(k)}.$$

Therefore we have:

$$z_0^{(k+1)} = z_0^{(k)} + (1/f_{00}) [p_0/\Delta t - \sum_{l=1}^n f_{0l} z_l^{(k)}]$$

Similarly from (2) above we have:

$$z_1^{(k+1)} = z_1^{(k)} + (1/f_{11}) [p_1/\Delta t - \sum_{l=0}^n f_{1l} z_l^{(k)}]$$

Therefore in general terms:

$$z_i^{(k+1)} = z_i^{(k)} + (1/f_{ii}) [p_i / \Delta t - \sum_{l=0}^n f_{il} z_l^{(k)}]$$

for $i = 0, 1, 2, 3, \dots, n$.

The necessary condition for this to work is $f_{ii} \neq 0$.

3.5.2 GAUSS-SEIDEL METHOD:

The example for splitting the matrix F is known as the "Gauss-Seidel" method or 'the method of successive displacements'.

Here we set: G = the lower triangular matrix which agrees with F in the elements below the main diagonal and J = the corresponding upper triangular matrix.

i.e. we have

$$G = \begin{bmatrix} 0 & 0 & 0 & \cdot & \cdot & \cdot & 0 \\ f_{10} & 0 & 0 & \cdot & \cdot & \cdot & 0 \\ f_{20} & f_{21} & 0 & \cdot & \cdot & \cdot & 0 \\ \cdot & \cdot & \cdot & \cdot & \cdot & \cdot & \cdot \\ \cdot & \cdot & \cdot & \cdot & \cdot & \cdot & \cdot \\ f_{n0} & f_{n1} & f_{n2} & \cdot & \cdot & f_{n,n-1} & 0 \end{bmatrix}$$

$$\text{and } J = \begin{bmatrix} 0 & f_{01} & f_{02} & f_{03} & \cdot & \cdot & \cdot & f_{0n} \\ 0 & 0 & f_{12} & f_{13} & f_{14} & \cdot & \cdot & f_{1n} \\ 0 & 0 & 0 & f_{23} & f_{24} & \cdot & \cdot & f_{2n} \\ \cdot & \cdot & \cdot & \cdot & \cdot & \cdot & \cdot & \cdot \\ \cdot & \cdot & \cdot & \cdot & \cdot & \cdot & \cdot & \cdot \\ 0 & 0 & 0 & 0 & 0 & 0 & 0 & 0 \end{bmatrix}.$$

and D is the diagonal matrix as in the Point-Jacobi method.

Now we split F as: $F = (D + G + J)$.

If we now set $M = D + G$ and $N = -J$ and by substituting this in the scheme: $M z^{(k+1)} = N z^{(k)} + p / \Delta t$, we can derive as before, the expression,

$$z_i^{(k+1)} = z_i^{(k)} + (1/f_{ii}) [p_i / \Delta t - \sum_{l=0}^n f_{il} z_l^{(k)}]$$

$i = 0, 1, 2, \dots$

3.5.3 RELAXATION METHOD:

In the third method which is called 'the point-successive-relaxation method', a numerical parameter α (alpha) is introduced and we refer to α as a 'relaxation parameter'.

As before we have,

$$M z^{(k+1)} = N z^{(k)} + p / \Delta t$$

But in this method, $M = (1/\alpha) [D + G]$

$$N = (1/\alpha) [(1-\alpha) D - \alpha J].$$

$$M = \begin{bmatrix} f_{00}/\alpha & 0 & 0 & \cdot & \cdot & 0 \\ 0 & f_{11}/\alpha & 0 & 0 & \cdot & \cdot & 0 \\ 0 & 0 & f_{22}/\alpha & 0 & \cdot & \cdot & 0 \\ \cdot & \cdot & \cdot & \cdot & \cdot & \cdot & \cdot \\ \cdot & \cdot & \cdot & \cdot & \cdot & \cdot & \cdot \\ 0 & 0 & 0 & 0 & 0 & 0 & f_{nn}/\alpha \end{bmatrix}$$

$$+ \begin{bmatrix} 0 & 0 & 0 & 0 & \cdot & \cdot & 0 \\ f_{10} & 0 & 0 & 0 & \cdot & \cdot & 0 \\ f_{20} & f_{21} & 0 & 0 & 0 & 0 & 0 \\ \cdot & \cdot & \cdot & \cdot & \cdot & \cdot & \cdot \\ \cdot & \cdot & \cdot & \cdot & \cdot & \cdot & \cdot \\ f_{n0} & f_{n1} & f_{n2} & \cdot & \cdot & \cdot & 0 \end{bmatrix}$$

and

$$N = \begin{bmatrix} ((1-\alpha)/\alpha)f_{00} & 0 & 0 & \cdot & \cdot & \cdot & 0 \\ 0 & ((1-\alpha)/\alpha)f_{11} & 0 & \cdot & \cdot & \cdot & 0 \\ 0 & 0 & ((1-\alpha)/\alpha)f_{22} & \cdot & \cdot & \cdot & 0 \\ \cdot & \cdot & \cdot & \cdot & \cdot & \cdot & \cdot \\ \cdot & \cdot & \cdot & \cdot & \cdot & \cdot & \cdot \\ 0 & 0 & 0 & 0 & \cdot & \cdot & ((1-\alpha)/\alpha)f_{nn} \end{bmatrix}$$

$$- \begin{bmatrix} 0 & f_{01} & f_{02} & f_{03} & \cdot & \cdot & \cdot & f_{0n} \\ 0 & 0 & f_{12} & f_{13} & f_{14} & \cdot & \cdot & f_{1n} \\ 0 & 0 & 0 & f_{23} & f_{24} & \cdot & \cdot & f_{2n} \\ \cdot & \cdot & \cdot & \cdot & \cdot & \cdot & \cdot & \cdot \\ \cdot & \cdot & \cdot & \cdot & \cdot & \cdot & \cdot & \cdot \\ 0 & 0 & 0 & 0 & 0 & 0 & 0 & 0 \end{bmatrix}$$

Substituting for M and N in

$M z^{(k+1)} = N z^{(k)} + p/\Delta t$, and simplifying we get:

$$z_0^{(k+1)} = z_0^{(k)} + (\alpha/f_{00}) [p_0/\Delta t - \sum_{l=0}^n f_{0l} z_l^{(k)}]$$

$$z_1^{(k+1)} = z_1^{(k)} + (\alpha/f_{11}) [p_1/\Delta t - (f_{10} z_0^{(k+1)}) - (\sum_{l=1}^n f_{1l} z_l^{(k)})]$$

.

. etc.,

Therefore the general expression would be:

$$z_i^{(k+1)} = z_i^{(k)} + (\alpha/f_{ii}) [p_i/\Delta t - \sum_{l=0}^{i-1} f_{il} z_l^{(k+1)} - \sum_{l=i}^n f_{il} z_l^{(k)}] .$$

for $i = 0, 1, 2, \dots$

The parameters that seem to play a critical role in this method are α (alpha) and f_{ij} . The relaxation parameter assumes the value between 0 and 1 when the system is said to be "under-relaxed" and between 1 and 2 when the system is said to be "over-relaxed". A careful choice of these parameters is the clue to the successful execution of the deconvolution procedure.

3.6 MODIFIED METHOD

Another method investigated in this study is a modified representation of the Point-Jacobi scheme.

We need to solve $P = F (Z \Delta t) \dots \dots \dots (3.6.1)$

Substituting $Z \Delta t = z \dots \dots (3.6.2)$ in (3.6.1), we get

$$P = F z \dots \dots \dots (3.6.3)$$

The modified scheme involves splitting the matrix F as:

$$F = (f_0 I + L) \text{ where } I \text{ is the Identity matrix}$$

L is the lower triangular matrix

From (3) we have: $P = (f_0 I + L) z$

$$\text{i.e. } f_0 I z = -L z + P$$

$$z^{(k+1)} = (-1/f_{00}) L z^{(k)} + (1/f_{00}) P \dots \dots (3.6.3a)$$

$$F = \begin{bmatrix} f_{00} & f_{01} & f_{02} & f_{03} & \cdot & \cdot & \cdot & f_{0n} \\ f_{10} & f_{11} & f_{12} & f_{13} & \cdot & \cdot & \cdot & f_{1n} \\ f_{20} & f_{21} & f_{22} & f_{23} & \cdot & \cdot & \cdot & f_{2n} \\ \cdot & \cdot & \cdot & \cdot & \cdot & \cdot & \cdot & \cdot \\ \cdot & \cdot & \cdot & \cdot & \cdot & \cdot & \cdot & \cdot \\ f_{n0} & f_{n1} & f_{n2} & f_{n3} & \cdot & \cdot & \cdot & f_{nn} \end{bmatrix}$$

$$\text{i.e. } F = f_{00} \begin{bmatrix} 1 & 0 & 0 & 0 & 0 & . & . & . & 0 \\ 0 & 1 & 0 & 0 & 0 & . & . & . & 0 \\ . & . & . & . & . & . & . & . & . \\ . & . & . & . & . & . & . & . & . \\ . & . & . & . & . & . & . & . & . \\ 0 & 0 & 0 & 0 & 0 & 0 & 0 & 0 & 1 \end{bmatrix} +$$

$$\begin{bmatrix} 0 & 0 & 0 & 0 & . & . & . & 0 \\ f_{10} & 0 & 0 & 0 & . & . & . & 0 \\ f_{20} & f_{21} & 0 & 0 & . & . & . & 0 \\ . & . & . & . & . & . & . & . \\ . & . & . & . & . & . & . & . \\ f_{n0} & f_{n1} & f_{n2} & . & . & . & f_{n,n-1} & 0 \end{bmatrix}$$

$$\text{i.e. } F = (f_{00} I - (-L))$$

Substituting this in:

$$M z^{(k+1)} = N z^{(k)} + P, \text{ we have:}$$

$$f_{00} \begin{bmatrix} 1 & 0 & 0 & 0 & 0 & . & . & . & 0 \\ 0 & 1 & 0 & 0 & 0 & . & . & . & 0 \\ 0 & 0 & 1 & 0 & 0 & . & . & . & 0 \\ . & . & . & . & . & . & . & . & . \\ . & . & . & . & . & . & . & . & . \\ . & . & . & . & . & . & . & . & . \\ 0 & 0 & 0 & 0 & 0 & . & . & 0 & 1 \end{bmatrix} \begin{bmatrix} z_0 \\ z_1 \\ z_2 \\ . \\ . \\ . \\ z_n \end{bmatrix}^{(k+1)} =$$

$$\begin{bmatrix} 0 & 0 & 0 & \cdot & \cdot & 0 \\ -f_{10} & 0 & 0 & \cdot & \cdot & 0 \\ -f_{20} & -f_{21} & 0 & \cdot & \cdot & 0 \\ \cdot & \cdot & \cdot & \cdot & \cdot & \cdot \\ \cdot & \cdot & \cdot & \cdot & \cdot & \cdot \\ \cdot & \cdot & \cdot & \cdot & \cdot & \cdot \\ -f_{n0} & -f_{n1} & \cdot & \cdot & \cdot & 0 \end{bmatrix} \begin{bmatrix} z_0^{(k)} \\ z_1 \\ z_2 \\ \cdot \\ \cdot \\ \cdot \\ z_n \end{bmatrix} + \begin{bmatrix} p_0 \\ p_1 \\ p_2 \\ \cdot \\ \cdot \\ \cdot \\ p_n \end{bmatrix} \dots\dots\dots(3.6.4)$$

i.e.

$$\begin{bmatrix} z_0^{(k+1)} \\ z_1 \\ z_2 \\ \cdot \\ \cdot \\ \cdot \\ z_n \end{bmatrix} = \begin{bmatrix} 0 & 0 & 0 & \cdot & \cdot \\ -f_{10}/f_{00} & 0 & 0 & \cdot & \cdot \\ -f_{20}/f_{00} & -f_{21}/f_{00} & 0 & \cdot & \cdot \\ \cdot & \cdot & \cdot & \cdot & \cdot \\ \cdot & \cdot & \cdot & \cdot & \cdot \\ \cdot & \cdot & \cdot & \cdot & \cdot \\ -f_{n0}/f_{00} & -f_{n1}/f_{00} & \cdot & \cdot & -f_{n,n-1}/f_{00} \end{bmatrix} \begin{bmatrix} z_0^{(k)} \\ z_1 \\ z_2 \\ \cdot \\ \cdot \\ \cdot \\ z_n \end{bmatrix} + \begin{bmatrix} p_0/f_{00} \\ p_1/f_{00} \\ p_2/f_{00} \\ \cdot \\ \cdot \\ \cdot \\ p_n/f_{00} \end{bmatrix}$$

$$= \begin{bmatrix} 0 & 0 & 0 & \dots & 0 \\ (-f_{10}/f_{00})z_0^{(k)} & 0 & 0 & \dots & 0 \\ (-f_{20}/f_{00})z_0^{(k)} & (-f_{21}/f_{00})z_1^{(k)} & 0 & \dots & 0 \\ \vdots & \vdots & \vdots & \ddots & \vdots \\ (-f_{n0}/f_{00})z_0^{(k)} & (-f_{n1}/f_{00})z_1^{(k)} & \dots & (-f_{n,n-1}/f_{00})z_{n-1}^{(k)} & 0 \end{bmatrix} + \begin{bmatrix} p_0/f_{00} \\ p_1/f_{00} \\ p_2/f_{00} \\ \vdots \\ p_n/f_{00} \end{bmatrix}$$

i.e.

$$z_0^{(k+1)} = (p_0/f_{00})$$

$$z_1^{(k+1)} = (-f_{10}/f_{00})z_0^{(k)} + p_1/f_{00}$$

$$z_2^{(k+1)} = (-f_{20}/f_{00})z_0^{(k)} + (-f_{21}/f_{00})z_1^{(k)} + p_2/f_{00}$$

.

:

$$z_n^{(k+1)} = (-f_{n0}/f_{00})z_0^{(k)} + (-f_{n1}/f_{00})z_1^{(k)} + (-f_{n2}/f_{00})z_2^{(k)}$$

$$+ \dots + (-f_{n,n-1}/f_{00})z_{n-1}^{(k)} + p_n/f_{00}.$$

$$\text{i.e. } z_i^{(k+1)} = [(-1/f_{00}) \quad f_{i1} z_1^{(k)}] + (p_i/f_{00})$$

for $i = 0, 1, 2, 3, \dots, n.$

In (3.6.3a), denote:

$$(-1/f_0) L = L^*$$

Suppose $z = L^* z + (1/f_{00}) P$ (z is a solution)

Look for $e^{k+1} = z - z^{(k+1)}$ (Error term)

$$\text{i.e. } e^{k+1} = (L^* z + (1/f_{00}) P) - (L^* z^{(k)} + (1/f_{00}) P)$$

$$\text{i.e. } e^{k+1} = L^* (z - z^{(k)}) = L^* e^k$$

$$\text{i.e. } \boxed{e^{(k+1)} = L^* e^k \quad \text{for all } k} \dots\dots\dots(3.6.5)$$

Equation (3.6.5) tracks the error in the iteration scheme.

$$\text{For } k = 0, e^1 = L^* e^0$$

$$\text{for } k = 1, e^2 = L^* e^1 = L^* (L^* e^0) = [L^*]^2 e^0$$

Proceeding in this pattern, we have:

$$e^k = L^* e^{k-1} = [(L^*)]^k e^0$$

The error can be calculated using:

$$\boxed{e^k = [(L^*)^k] e^0 \quad \text{for } k = 1, 2, 3, 4, \dots}$$

In matrix notation,

$$L^* = (-1/f_{00}) \begin{matrix} 0 & 0 & 0 & \cdot & \cdot & \cdot & \cdot & 0 \\ f_{10} & 0 & 0 & \cdot & \cdot & \cdot & \cdot & 0 \\ f_{20} & f_{21} & 0 & \cdot & \cdot & \cdot & \cdot & 0 \\ f_{30} & f_{31} & f_{32} & 0 & \cdot & \cdot & \cdot & 0 \\ \cdot & \cdot & \cdot & \cdot & \cdot & \cdot & \cdot & \cdot \\ \cdot & \cdot & \cdot & \cdot & \cdot & \cdot & \cdot & \cdot \\ \cdot & \cdot & \cdot & \cdot & \cdot & \cdot & \cdot & \cdot \\ f_{n0} & f_{n1} & f_{n2} & \cdot & \cdot & \cdot & f_{n,n-1} & 0 \end{matrix}$$

e^0 is a vector.

As k approaches infinity, e^k approaches the null vector for any initial vector e^0 , if and only if $[L^*]^k$ approaches 0 as k approaches infinity.

Let the components of e^0 be: e^{0p} and the elements of

$[(L^*)]^k$ are:

$$l_{jp}^{(k)} = f_{jp}^{(k)} / f_{00}$$

Then

$$\boxed{[e^k]_j = l_{jp}^{(k)} e^{0p}} \dots\dots\dots(3.6.6)$$

for $j = p$ and $j < p$, elements are zero

for $j = p = 0$, $f_{jp} \neq 0$

(3.6.6) is used to find the error at every iterative step.

(3.6.3a) gives z . But what we are looking for is Z .

i.e. Z can be calculated from $Z \Delta t = z$

i.e. $Z = (z / \Delta t)$ where Z is the impulse response function.

The main advantage of this method is that it will allow us to track down the error at the end of each iteration step.

3.7 Further Modification of the Previous Method

In this section we report a further modification to the previous scheme such that the method yields faster convergence.

Again as before, $P = F Z \Delta t \dots\dots\dots(3.7.1)$

substituting $Z \Delta t = z$ in (3.7.1), we get

$$P = F z \dots\dots\dots(3.7.2)$$

We now split F as $F = (D + L)$ where D is the diagonal

matrix and L is the lower triangular matrix.

Therefore (3.7.2) becomes:

$$P = (D + L) z$$

i.e. $D z_{k+1} = -L z_k + P$

$$D^{-1} D z_{k+1} = -D^{-1} L z_k + D^{-1} P$$

i.e. $z_{k+1} = (-D^{-1} L) z_k + D^{-1} P \dots\dots\dots(3.7.3)$

$$\text{Define } z = E y \dots\dots\dots(3.7.4)$$

where:

$$E = \begin{pmatrix} \epsilon^n & 0 & 0 & \dots & \dots & \dots & 0 \\ 0 & \epsilon^{n-1} & 0 & \dots & \dots & \dots & 0 \\ 0 & 0 & \epsilon^{n-2} & \dots & \dots & \dots & 0 \\ \dots & \dots & \dots & \dots & \dots & \dots & \dots \\ \dots & \dots & \dots & \dots & \dots & \dots & \dots \\ 0 & 0 & 0 & \dots & \dots & \dots & \epsilon^0 \end{pmatrix}$$

Now (3.7.3) becomes

$$E Y_{k+1} = (-D^{-1} L) E Y_k + D^{-1} P$$

$$(E^{-1} E) Y_{k+1} = E^{-1} (-D^{-1} L) E Y_k + E^{-1} (-D^{-1} P)$$

$$\text{i.e. } \boxed{Y_{k+1} = (E^{-1} \hat{L} E) Y_k + E^{-1} \hat{P}} \dots\dots\dots(3.7.5)$$

where

$$(-D^{-1} L) = \hat{L}$$

$$\text{and } D^{-1} P = \hat{P}$$

Therefore the matrix $-D^{-1} L$ becomes equal to:

$$(-D^{-1} L) = \begin{bmatrix} (-1/f_{00}) & 0 & 0 & \dots & \dots & \dots & 0 \\ 0 & (-1/f_{11}) & 0 & \dots & \dots & \dots & 0 \\ 0 & 0 & (-1/f_{22}) & 0 & \dots & \dots & \dots \\ \dots & \dots & \dots & \dots & \dots & \dots & \dots \\ \dots & \dots & \dots & \dots & \dots & \dots & \dots \\ 0 & 0 & 0 & \dots & \dots & 0 & (-1/f_{nn}) \end{bmatrix}$$

$$\begin{bmatrix} 0 & 0 & 0 & \dots & \dots & \dots & \dots & \dots & 0 \\ f_{10} & 0 & 0 & \dots & \dots & \dots & \dots & \dots & 0 \\ f_{20} & f_{21} & 0 & \dots & \dots & \dots & \dots & \dots & 0 \\ \dots & \dots & \dots & \dots & \dots & \dots & \dots & \dots & \dots \\ \dots & \dots & \dots & \dots & \dots & \dots & \dots & \dots & \dots \\ \dots & \dots & \dots & \dots & \dots & \dots & \dots & \dots & \dots \\ \dots & \dots & \dots & \dots & \dots & \dots & \dots & \dots & \dots \\ f_{n0} & f_{n1} & f_{n2} & \dots & \dots & \dots & \dots & f_{n,n-1} & 0 \end{bmatrix}$$

$$\begin{bmatrix} 0 & 0 & 0 & \dots & \dots & \dots & \dots & \dots & 0 \\ (-f_{10}/f_{11}) & 0 & 0 & \dots & \dots & \dots & \dots & \dots & 0 \\ (-f_{20}/f_{22}) & (-f_{21}/f_{22}) & 0 & \dots & \dots & \dots & \dots & \dots & 0 \\ \dots & \dots & \dots & \dots & \dots & \dots & \dots & \dots & \dots \\ \dots & \dots & \dots & \dots & \dots & \dots & \dots & \dots & \dots \\ \dots & \dots & \dots & \dots & \dots & \dots & \dots & \dots & \dots \\ \dots & \dots & \dots & \dots & \dots & \dots & \dots & \dots & \dots \\ (-f_{n0}/f_{nn}) & (-f_{n1}/f_{nn}) & \dots & \dots & \dots & \dots & (-f_{n,n-1}/f_{nn}) & \dots & 0 \end{bmatrix}$$

Pre-multiplying and post multiplying $(-D^{-1} L)$ by E^{-1} and E respectively, we get

$$[E^{-1} (-D^{-1} L) E] = \begin{bmatrix} 0 & 0 & 0 & \dots & 0 \\ (-f_{10}/f_{11}) \epsilon^1 & 0 & 0 & \dots & 0 \\ (-f_{20}/f_{22}) \epsilon^2 & (-f_{21}/f_{22}) \epsilon^1 & 0 & \dots & 0 \\ \vdots & \vdots & \vdots & \vdots & \vdots \\ (-f_{n0}/f_{nn}) \epsilon^n & (-f_{n1}/f_{nn}) \epsilon^{n-1} & \dots & (-f_{n,n-1}/f_{nn}) \epsilon^1 & 0 \end{bmatrix}$$

Now pre-multiplying (D^{-1}) by (E^{-1}) we get:

$$E^{-1} D^{-1} = \begin{bmatrix} (1/\epsilon^n)(1/f_{00}) & 0 & \dots & 0 \\ 0 & (1/\epsilon^{n-1})(1/f_{11}) & \dots & 0 \\ \vdots & \vdots & \vdots & \vdots \\ \vdots & \vdots & \vdots & \vdots \\ 0 & 0 & \dots & (1/f_{nn}) \end{bmatrix}$$

Substituting for $E^{-1} (-D^{-1} L) E$ and $E^{-1} D^{-1}$ in the equation (3.7.5) we get:

$$\begin{bmatrix} Y_0 \\ Y_1 \\ Y_2 \\ \vdots \\ \vdots \\ \vdots \\ Y_n \end{bmatrix}^{(k+1)} = \begin{bmatrix} 0 & 0 & \dots & 0 \\ (-f_{10}/f_{11}) \epsilon^1 & 0 & \dots & 0 \\ (-f_{20}/f_{22}) \epsilon^2 & 0 & \dots & 0 \\ \vdots & \vdots & \vdots & \vdots \\ \vdots & \vdots & \vdots & \vdots \\ \vdots & \vdots & \vdots & \vdots \\ (-f_{n0}/f_{nn}) \epsilon^n & (-f_{n1}/f_{nn}) \epsilon^{n-1} & \dots & 0 \end{bmatrix} \begin{bmatrix} Y_0 \\ Y_1 \\ Y_2 \\ \vdots \\ \vdots \\ \vdots \\ Y_n \end{bmatrix}^{(k)}$$

$$+ \begin{bmatrix} 1/(\epsilon^n f_{00}) & 0 & . & . & 0 & p_0 \\ 0 & 1/(\epsilon^{n-1} f_{11}) & . & . & 0 & p_1 \\ 0 & 0 & 1/(\epsilon^{n-2} f_{22}) & . & . & p_2 \\ . & . & . & . & . & . \\ . & . & . & . & . & . \\ . & 0 & 0 & . & (1/f_{nn}) & p_n \end{bmatrix}$$

Simplifying the above matrices, we get:

$$Y_0^{(k+1)} = (p_0 / (\epsilon^n f_{00}))$$

$$Y_1^{(k+1)} = (-f_{10} \epsilon^{1/f_{11}}) Y_0^{(k)} + (1 / (\epsilon^{n-1} f_{11})) p_1$$

.
.

$$Y_n^{(k+1)} = (-f_{n0} \epsilon^{n/f_{nn}}) Y_0^{(k)} + (-f_{n1} \epsilon^{n-1/f_{nn}}) Y_1^{(k)} \\ + \dots + (-f_{n,n-1} \epsilon^{1/f_{nn}}) Y_{n-1}^{(k)} + p_n / f_{nn}$$

This set of equations can be written in the summation form as:

$$Y_i^{(k+1)} = \left[\sum_{l=0}^{i-1} (-f_{il} \epsilon^{i-1/f_{ii}}) Y_l^{(k)} \right] + p_i / (\epsilon^{n-i} f_{ii})$$

for $i = 0, 1, 2, 3, \dots, n$ and $f_{ii} \neq 0$

.....(3.7.6)

From (3.7.6), we get y . But $z = E y$.

$$\text{i.e. } Z \Delta t = E y \quad (\text{since } z = Z \Delta t)$$

$$Z = (E y / \Delta t)$$

where Z is the impulse response function.

The E-Matrix here defines a parameter "Epsilon".

4. RESULTS AND DISCUSSIONS

The performances of the various numerical approximation methods discussed in the previous sections were evaluated and compared using two models with known characteristics. These are:

1. an RC Filter network and
2. a 3-element Windkessel model.

4.1 RC Filter

The RC network model was chosen such that the time constant $RC = 1$ and the value of the compliance was 0.01. The input considered is a half-sine wave given by:

$$\begin{aligned} f(t) &= \sin(t) + A && \text{for } 0 < t < \pi \text{ (}\pi = 3.1415\text{)} \\ &= 0 && \text{otherwise} \end{aligned} \quad \dots\dots\dots(4.1)$$

where A is a DC component. The impulse response function of the network is assumed to be:

$$h(t) = (1/C) e^{-t/a} \quad \dots\dots\dots(4.2)$$

so that the convolution of $f(t)$ and $h(t)$ would yield the output $p(t)$, given by

$$\begin{aligned} p(t) &= 0 && \text{for } t < 0 \\ &= (1/2C) [\sin(t) - \cos(t) + e^{-t} + A(e^t - 1)] \\ &&& \text{for } 0 < t < \pi \text{ (}\pi = 3.1415\text{)} \\ &&& \dots\dots\dots(4.3) \\ &= (1/2C) [A e^{\pi} + e^{-\pi} - 1] && \text{for } t < \pi \end{aligned}$$

The input and output time histories are illustrated in figure (1). Utilizing these data, the impulse response function was computed by deconvolving the two sets of

data, using the different methods described in the previous sections. The impulse response function of the model is a negative exponential function as given by equation (4.2), with the initial value at $t = 0$ to be the inverse of compliance value. The results of analysis of the application of direct deconvolution method, also termed here as the "conventional method" for ease of distinction, are presented in figure(2). The instability of the impulse response function at $t = (T/2)$ (where $T =$ total signal duration) is presumably due to insufficient sampling rate criteria and needs to be more closely investigated.

The start of deconvolution was set at time index $t = 3$ to avoid division by a small initial value (see equation set 3.2.1). The impulse response function follows the expected negative exponential function according to equation (4.2). Although the result clearly indicates that for well defined signals as in example (1) the direct numerical procedure works fairly satisfactorily, the procedure has certain inherent features which make it difficult for application in many experimental situations especially when the data are corrupted by the presence of even a slight amount of noise. However the method should not be lightly regarded as it does provide satisfactory results under certain ideal conditions. The model has been successfully used in several biological applications (Segre, 1967).

Examining the equation set 3.2.1, one would notice that two

important constraints emerge. These are (1) the input value at $t = 0$ can never be zero, and (2) the time between samples (or the sampling rate) plays a critical role in the accurate estimation of the impulse response function. When the input value is zero at $t = 0$, one would be tempted to consider the next non-zero value as the start point for deconvolution. The effect of doing this is demonstrated later on which indicates the discrepancies in the magnitudes and shape of the impulse response function. In many practical situations, this will play a critical role as in the case of the arterial system in which the input function i.e. the aortic flow assume zero or near-zero values. There is another source of error which arises from the choice of the sampling rate. In general, increasing the sampling interval will increase the error in the impulse response function and an optimum sampling interval need to be selected. (M.E.Valentinuzzi, E.M.Montalado Volache, 1975).

The direct method was applied to the measured excitation and response data obtained from an RC network. The input, $f(t)$ and the output, $p(t)$ time histories are illustrated in figure (3). The R and C characteristics of the filter were chosen to be 13k Ohms and 13micro-Farads respectively. The impulse response function computed by the direct method is illustrated in figure(4). Deconvolution was initiated at time index $t = 5$. Although the exponential characteristics of the impulse response function are evident, the method does introduce some fluctuations in the computed function. Both

the start point and the sampling interval contribute to these fluctuations.

A second procedure, the point-Jacobi method, was investigated for computing the impulse response function of the RC Filter network from the measured data. Although theoretically this method represents a better solution with convergence properties well suited to the analysis of certain class of linear systems, the method becomes even more inefficient for the case when the initial value happens to be zero. Any shift in the start point gives rise to highly distorted and meaningless impulse response function as indicated in figure(5). Increasing the number of iterations does not yield any improvement in the computed function.

The third method that has potential use in the deconvolution procedure is the relaxation method described in the previous section. The method introduces a relaxation parameter, "alpha" to control the stability of the iterative solution of the deconvolution algorithm. Proper choice of alpha is the key to the successful application of the method to practical problems. The system is considered "under relaxed" for values of alpha between 0 and 1 and "over relaxed" for values between 1 and 2. If the value "alpha" is equal to 1 the method will reduce to the Gauss-Seidel procedure. The method however still requires the initial value of the input to be non-zero. The impulse response function of the RC network (analytical model) obtained by Gauss-Seidel method

is illustrated in figure(6), which has an initial peak, gradually following the expected exponential curve. The instability at $t = T/2$ is still present.

The parameters that seem to influence the accuracy of the impulse response function computed by the relaxation methods are (1) the relaxation parameter, (2) the start point for deconvolution and (3) the number of iterations. The last parameter, i.e. the number of iterations, k , is obviously variable up till the point at which the solution converges. When this is reached, increasing the number of iterations does not in any way affect the final solution already obtained. In the case of the RC network, it required less than 25 iterations to obtain the necessary impulse response function. This is illustrated in figures (7) and (8) in which k is increased from 25 to 100 iterations with the same relaxation parameter. The results are identical.

The relaxation parameter is a key variable and has a strong influence on the convergence properties of the deconvolution solution. The effect of varying the relaxation parameter is given in figures (9) and (10) in which the parameter is varied from 0.1 to 0.5 and the results are seen to be grossly different at the end of 25 iterations.

Finally, the influence of the start point is critical in the relaxation procedure. Ideally the method requires the initial value of the input time history to be a non-zero value. This cannot be always satisfied especially in the case of the

arterial system. The effect of selecting the next non-zero value as the initial value can give rise to serious errors especially if noise is present in the data. The error will progressively increase as t increases. For a simple analytical model, the difference may not be significant as shown in figures (11) and (12) for the case of the RC Filter network. However the results of figures (11) and (12) provide us some insight in to the way the error might build up.

In deriving the impulse response function by numerical procedure, it would be extremely useful to be able to characterize and track down the error at the end of each iteration loop. In an attempt to do this, the Point-Jacobi method was modified to account for the error at the end of a given number of iterations.

The mathematical error representation implemented in the method is described in the previous section. The procedure needs a set of initial values for the impulse response function. In order to satisfy this, the impulse response function was computed by the direct method, the results of which were used as the initial values. When applied to the RC network model, the procedure resulted in very large fluctuations in the impulse response function with even much larger error magnitudes. Increasing the number of iterations to as large as 3000 did not yield the required convergence. A zero-array initial values did not improve the impulse response function. This method is also very sensitive

to the initial value of the input waveform. Therefore the method was not pursued further.

The effect of division by the sampling interval on the impulse response function is seen to be another adverse factor in achieving the accurate estimates of the impulse response function using the relaxation method. If the values become too small following the division, the method becomes very sensitive giving rise to large errors as it propagates with increasing t . In order to minimize these effects, the relaxation method was remodified such that the division by sampling interval was eliminated during the course of iteration. The final result obtained at the end of the given number of iterations was divided by the sampling interval after completion of all iterations. A new parameter "Epsilon" was introduced in the iteration procedure, the structure of which is described in the previous section. The method however is extremely sensitive to the start point of deconvolution. This is illustrated in figure(13) in which the impulse response function of the RC network begins to oscillate with increasing amplitudes.

When the start points were changed to 3, 4 and 5, the method generated reasonable impulse response functions as demonstrated in figures (14), (15) and 16.

To obtain insight in to the stability of the method to experimental data, the excitation and response data generated by the RC network model were subjected to the modified

procedure. The results are given in figure(17) which should be compared with figure(4). The results resemble closely the true impulse response function although the presence of sinusoidal oscillations in the computed impulse response function is intriguing. The latter needs further investigations.

4.2 WINDKESSEL MODEL

The major aim of the current project is to develop appropriate numerical approximation methods for the deconvolution of arterial pressure and flow waveforms in circulatory dynamics. This would enable us to compute the arterial impulse response function which would otherwise have to be computed by frequency domain transformation methods (Laxminarayan et al 1978). The advantages and limitations of the time domain approach are summarized in the earlier sections (Laxminarayan et al 1978). In an effort to evaluate the performances of the various numerical procedures described in the previous section for the arterial system, data generated from a 3-element Windkessel model were analysed. The latter serves as a good model of the arterial system under control conditions (Westerhof et al 1979). The model consists of a resistance R_c (equal to the characteristic impedance of the arterial system) in series with a parallel combination of another resistance R_p (representing the peripheral resistance) and a capacitor C (representing the total arterial compliance). The model parameters chosen were:

$$R_p = 2969 \text{ g.cm}^{-4} \text{ s}^{-1}$$

$$R_C = 500 \text{ g.cm}^{-4} \text{ s}^{-1}$$

$$\text{and } C = 0.00002 \text{ g}^{-1} \cdot \text{cm}^4 \text{ s}^2.$$

The aortic pressure and flow generated by the model are shown in figure (18) and figure (19).

The application of the deconvolution procedure to the Windkessel data is severely hampered by the negligibly small flow values. Division by the small value at $t = 0$, will give rise to large errors in the impulse response function and the magnitude of the error progressively increases, as t increases. This effect is typically seen in the direct as well as in the Jacobi and Gauss-Seidel methods. Figure(20) illustrates the impulse response function computed by direct methods. The application of relaxation procedures was found to suffer from the same flaws. When the system was under relaxed, it was noted that the system became extremely sensitive to the start point whereas the over-relaxation yielded extremely noisy impulse response functions. The latter also seemed to indicate that the sample interval is critical. In both cases it was not possible to recover the impulse response function from deconvolution procedures.

A notable point however is that an optimum choice of the start point, sampling interval and the relaxation parameter need to be made in order to obtain meaningful impulse response function. This aspect of the study needs further investigations.

The modified relaxation method, on the other hand, seems to

be more effective in extracting the impulse response function. It is interesting to note that the parameter "Epsilon" has a strong influence on the convergence properties, yet its magnitude did not have a significant effect on the computer runs. Several choices of "Epsilon" between 0 and 1 all produced roughly the same output and convergence rate when applied to the data. The start point for deconvolution is again an important parameter. In the present example different start points were tried out.

Figure(21) illustrates the results of deconvolution with the start point set at $t = 34$ and the values of Epsilon being 0.5. The error begins to oscillate with increasing amplitudes as t increases. In this example the iteration procedure was continued up to $k = 2000$.

Figure(22) illustrates the impulse response function obtained when the deconvolution procedure was activated at $t = 44$ which corresponds to a point in the rising segment of the "systolic" part. The exponential decay part of the impulse response function is to be expected. By extrapolating the exponential decay to time $t = 0$, one can estimate the total arterial compliance. It seems that the modified relaxation method represents a better technique for computing the system impulse response function. The computed function looks still noisy, and it is worthwhile investigating mathematical smoothing applications to the measured data prior to subjecting these to the deconvolution procedure. Given the nature of the data as the aortic

pressure and aortic flow, it is imperative that one should thoroughly investigate methods to overcome the effects of choosing the non-zero start point at time index which does not correspond to zero time in reality.

REFERENCES

1. J.S. Bendat, A.G. Piersol (1971), "Random data: Analysis and Measurement Procedures", Wiley, N.Y., London.
2. D.H. Bergel (1972), "Cardiovascular Dynamics", London and New York.
3. S.D. Conte, Carl de Boor, "Elementary Numerical Analysis, an algorithmic approach", Second edition, McGraw - Hill Kogakusha, Ltd.
4. S. Laxminarayan (1979 a), "Calculation of Forward and Backward Waves in the arterial system", Med. & Biol. Eng. & Comp. 17, 130.
5. S. Laxminarayan, R. Laxminarayan, G.J. Langewaters, A.V.D. Vos (1979 b), "Computing the Total arterial Compliance of the Arterial System from its input - impedance", Med. & Biol. Eng. & Comp. 17, 623 - 628.
6. S. Laxminarayan, R. Laxminarayan (1980), "Linear Systems Analysis Applications in the Study of Arterial Hemodynamics", Bio - Fluid Mechanics, Ed. Schenk, Plenum Publishers, N.Y., 2, 343 - 368.
7. S. Laxminarayan, P. Sipkema, N. Westerhof (1978), "Characterization of the Arterial System in the Time Domain", IEEE Trans. on Biomedical Engineering, BME - 25, 2, 177 - 185.
8. G. Segre (1967), Compartmental Models in the Analysis of Intestinal Absorption", Protoplasma, 63, 328 - 335.
9. G. Strang, "Linear Algebra and its Applications", Academic Press, N.Y., London, 1980.
10. M.E. Valentinuzzi, E.M. Montalado Volache (1975), "Discrete Deconvolution", Medical and Biological Engineering, 123 - 125.
11. G.C. Van Den Bos, N. Westerhof, G. Elzinga, P. Sipkema (1976), "Reflections in the Systemic Arterial System: Effects of Aortic & Carotid Occlusion", Cardiovas. Res., Vol. 10, 565 - 573.
12. N. Westerhof, P. Sipkema, G. Elzinga, J.P. Murgo, J.P. Giolma (1979), "Arterial Impedance, In: Quantitative Cardiovascular Studies", Ed: Hwang, Gross, Patel, University Park Press, Baltimore, 111 - 150.

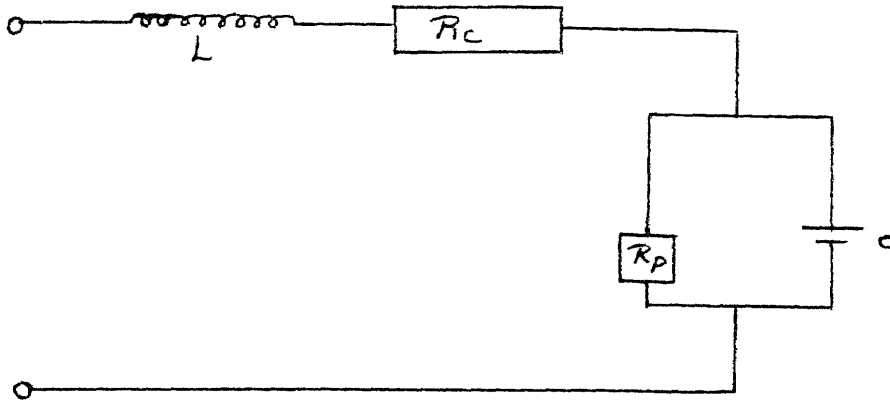


Figure A.1 WINDKESSEL MODEL

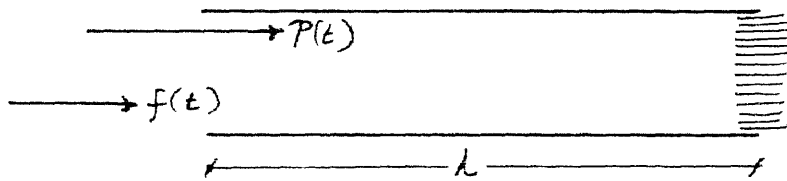


Figure A.2 UNIFORM TUBE MODEL

FIGURE 1

Input $f(t)$ and output $p(t)$ of a simple RC Filter network. $RC = 1$, $C = 0.01$. The total number of samples considered in $f(t)$ and $p(t)$ is, $N = 100$ so that one time index on the X-axis represents $(\pi/50)$ units. The total duration T of the data is $2(\pi)$.

INPUT-OUTPUT TIME HISTORIES

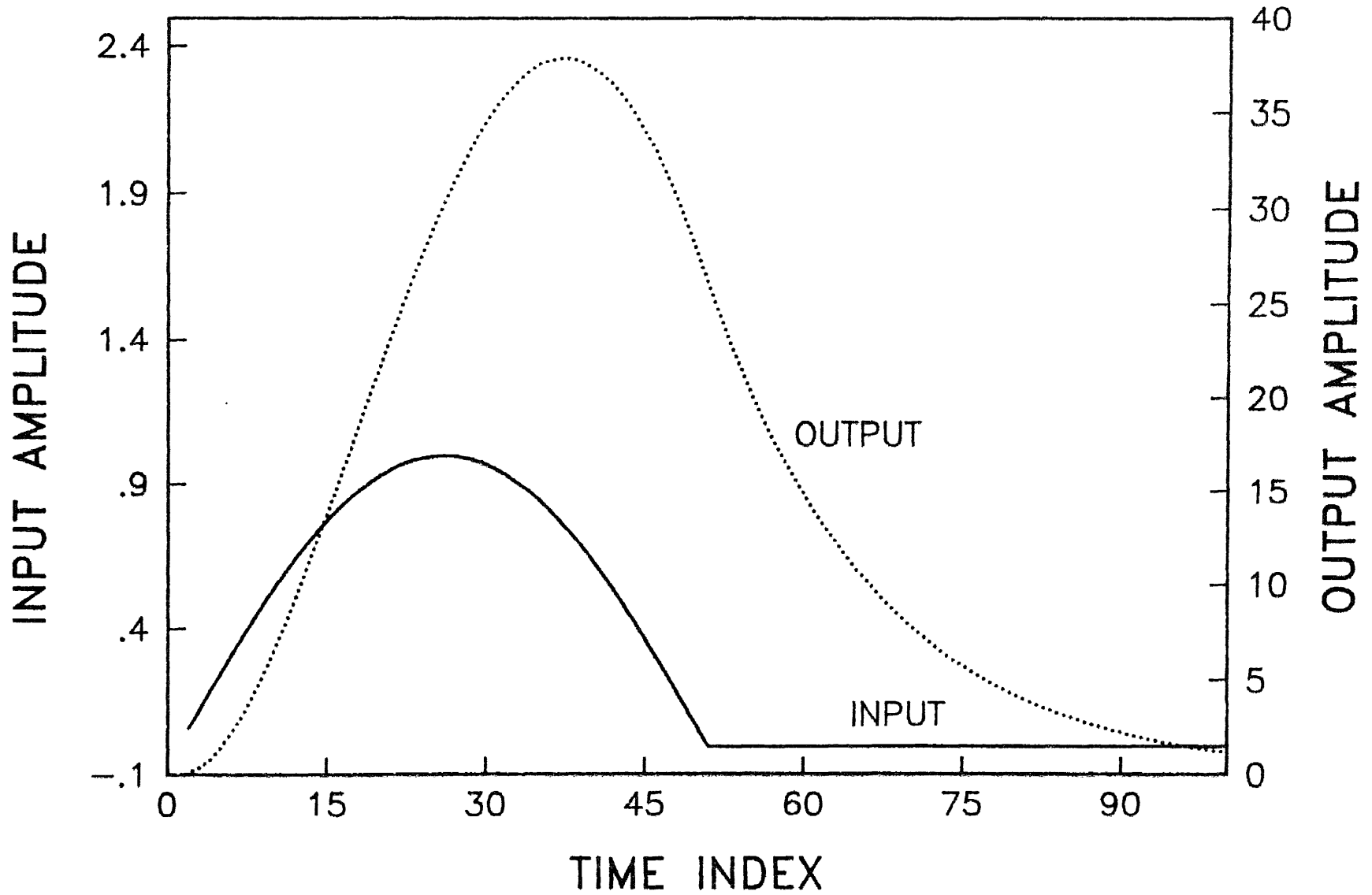


Fig. 1

FIGURE 2

Impulse response function (IRF) of the RC Filter network of figure(1). The direct deconvolution procedure was initiated at time index $t = 3$. This was necessary in order to avoid division by zero at $t = 0$.

RC NETWORK, $RC=1$, $C=.01$, $DC=0$, $N=101$

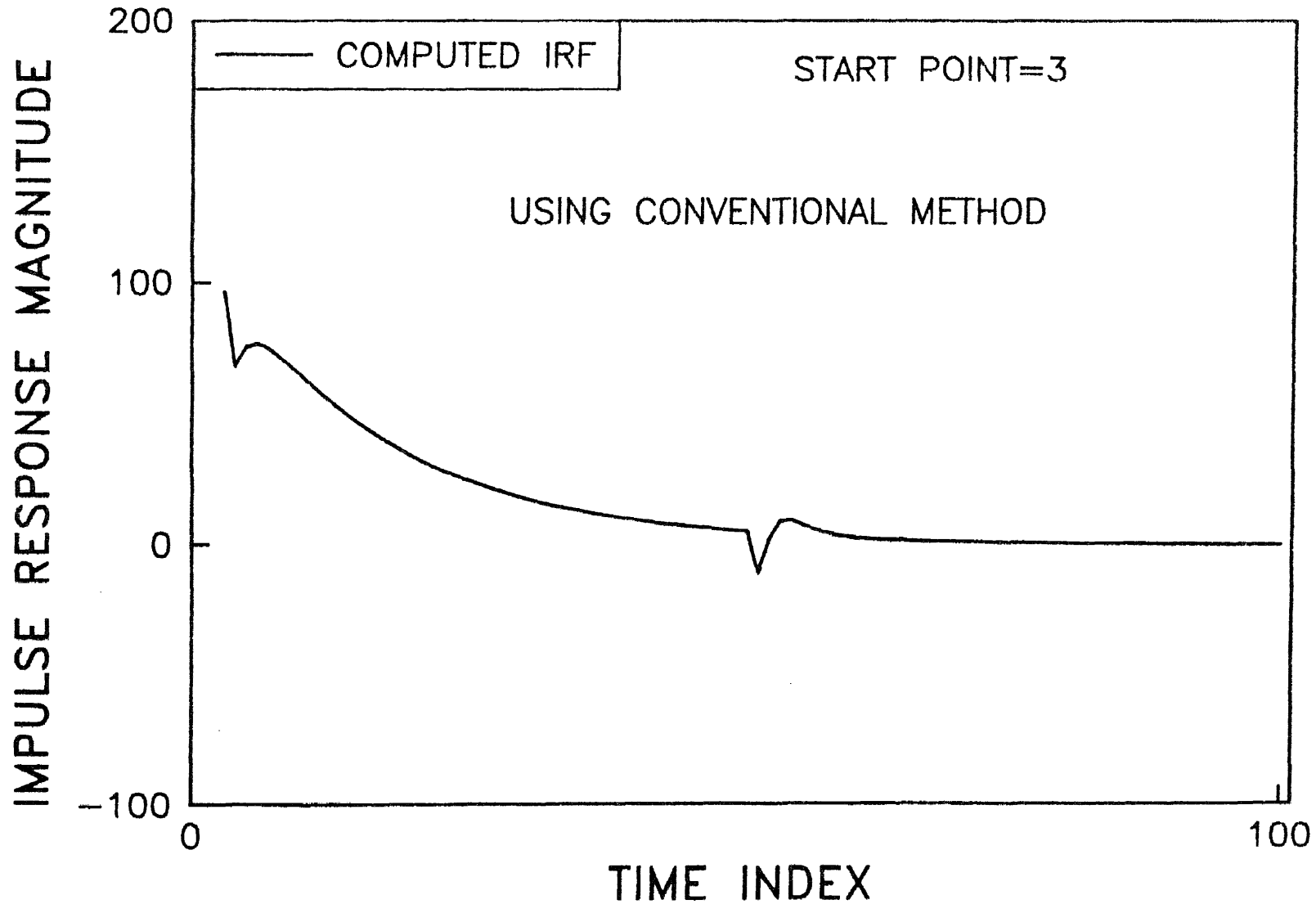


Fig. 2

FIGURE 3

Measured data from an RC network. $R = 13k$ ohms and $C = 13$ Farads. $f(t)$ and $p(t)$ represent the input and output time histories respectively. The time index of the X-axis is defined similar to the analytical example of figure(1).

RC NETWORK, MEASURED DATA FROM THE CIRCUIT

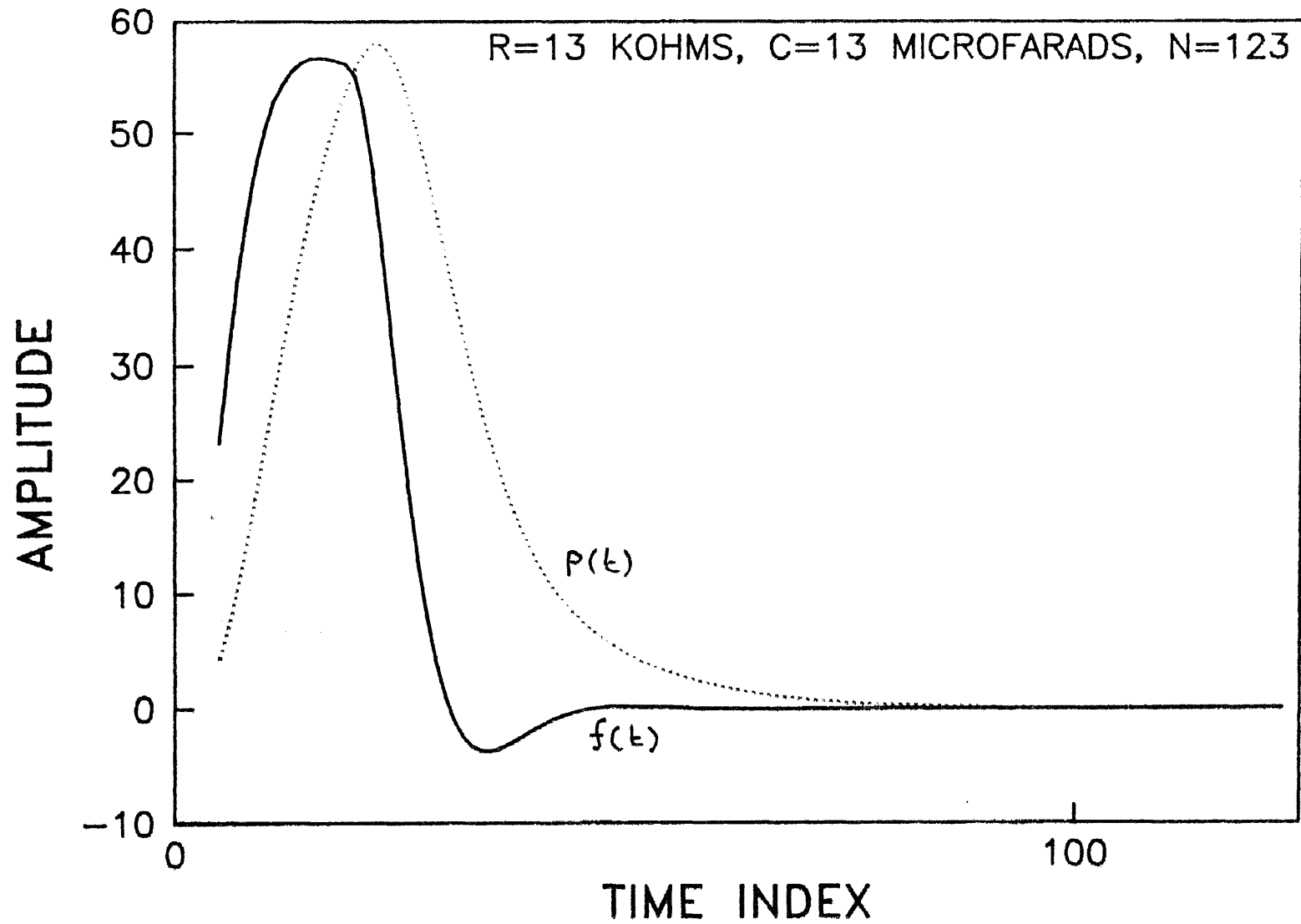


Fig. 3

FIGURE 4

Impulse response function of the RC network of figure(3)
computed from the measured signals.

R=13 KOHMS, C=20 MFARADS, N=123, START=5

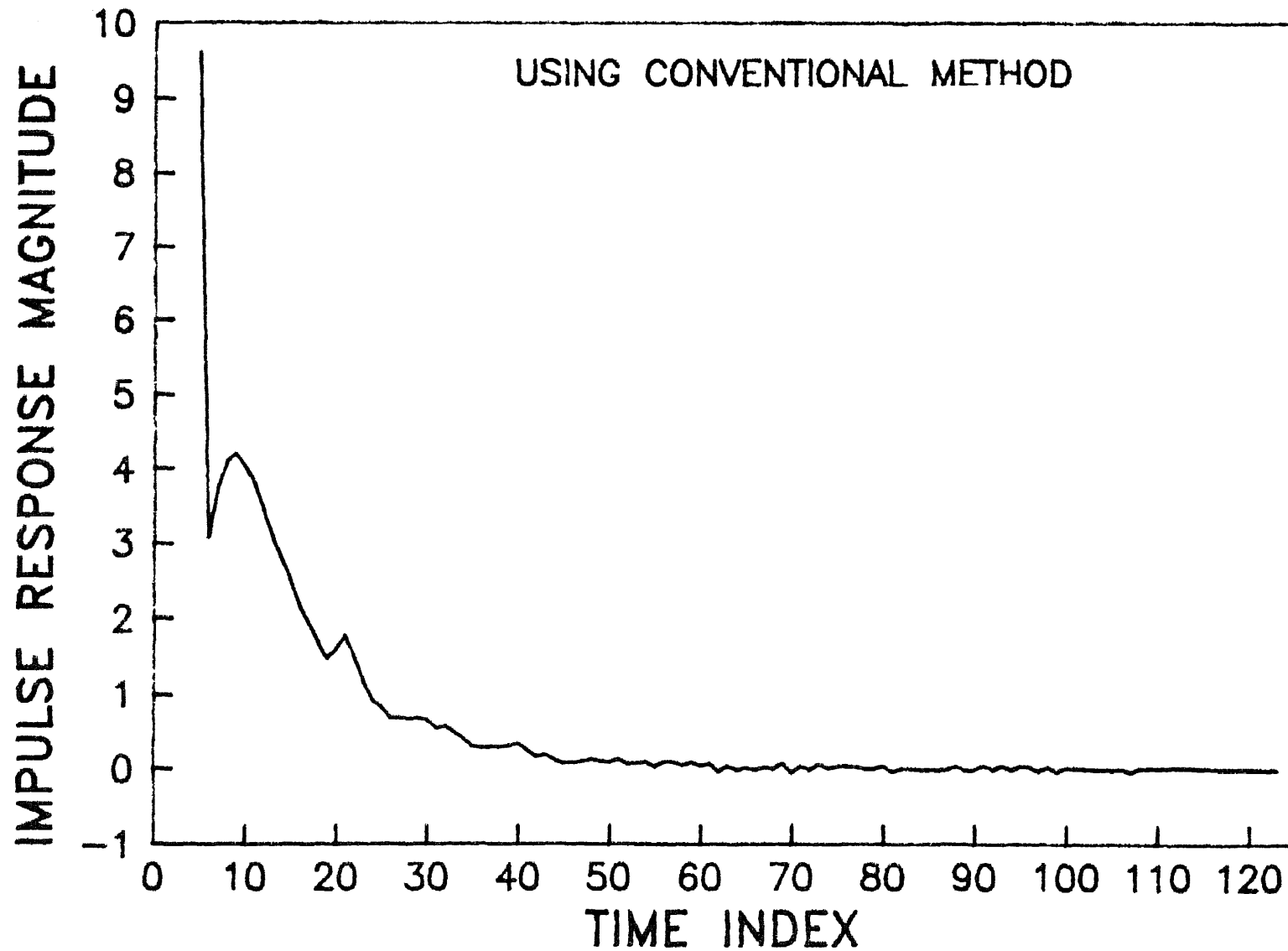


Fig. 4

FIGURE 5

Impulse response function of the RC network computed from the measured input and output time histories. Deconvolution was performed by Point-Jacobi method.

FILE=ITT11, START=10, # OF ITERATIONS=4

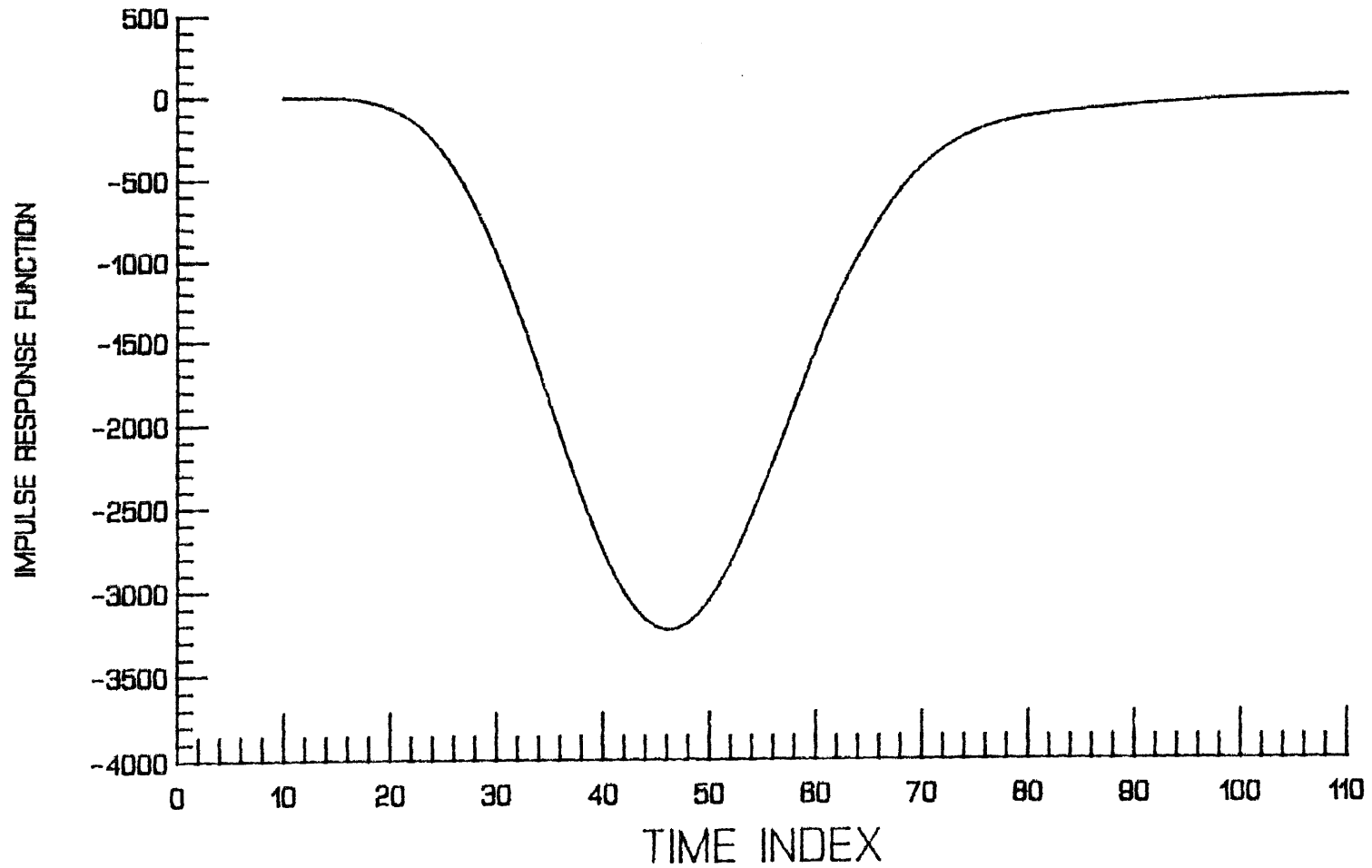


Fig. 5

FIGURE 6

Impulse response function of the RC Filter network using the Gauss-Siedal method. Deconvolution was initiated at time index $t = 2$ with relaxation parameter set equal to 1. Extrapolation of the exponential curve to time index $t = 0$ yields a value equal to the inverse of the compliance as predicted by the theoretical model.

RC NETWORK, $RC=1$, $C=.01$

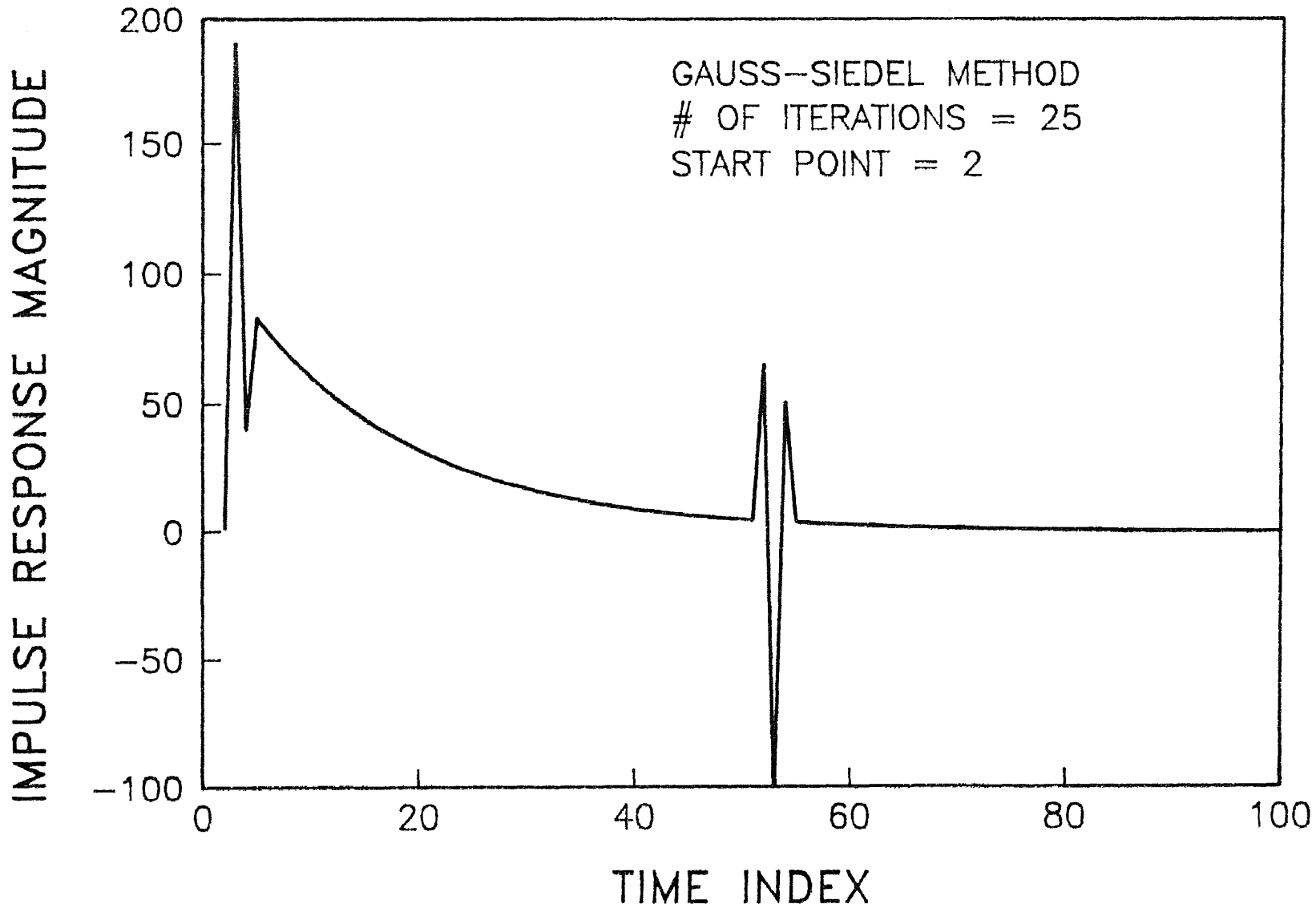


Fig. 6

FIGURE 7

Impulse response function of the RC network computed by relaxation method. Number of iterations is 25 with the relaxation parameter 0.5.

RC FILTER, $RC=1$, $C=.01$

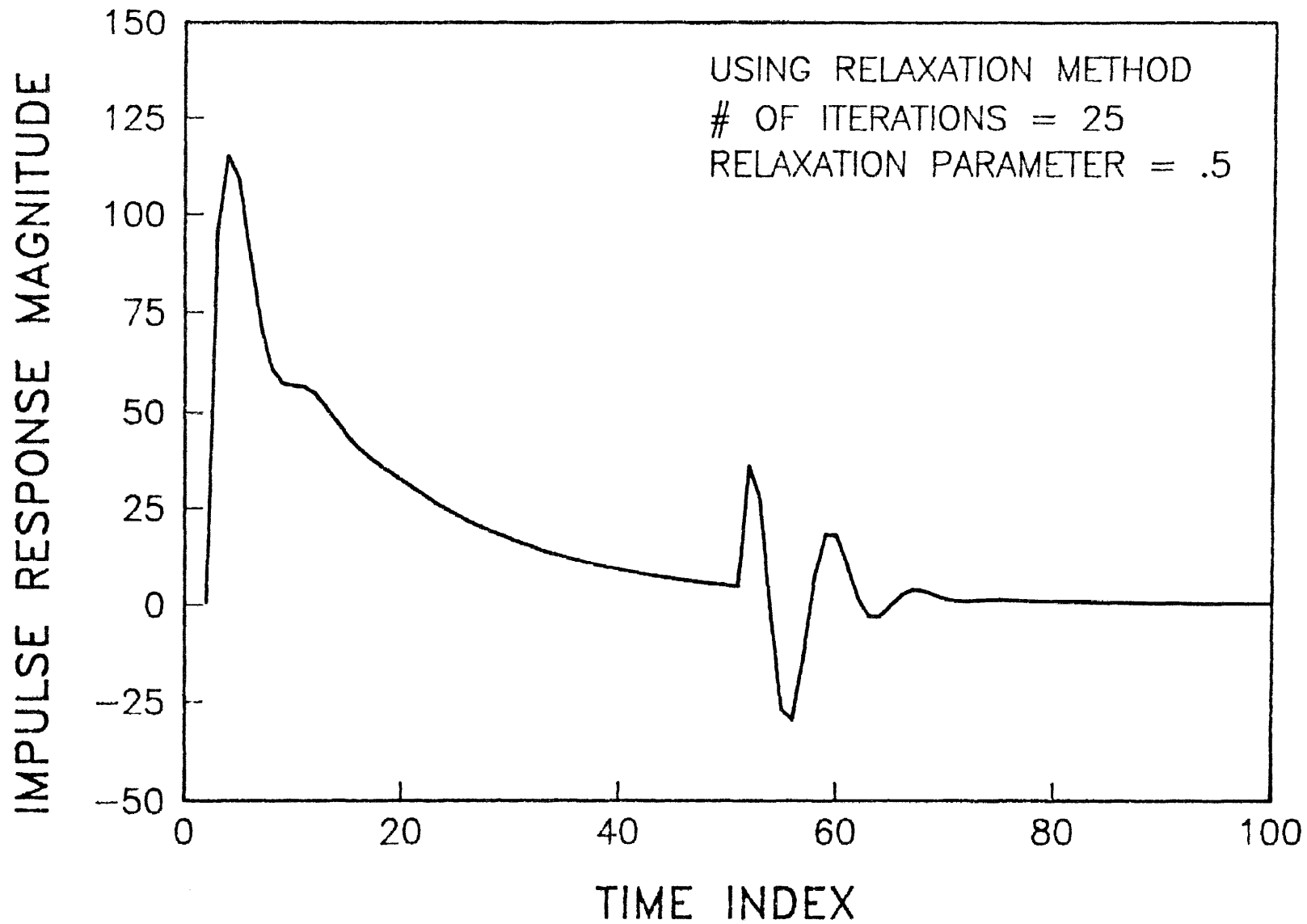


Fig. 7

FIGURE 8

Impulse response function of the RC network computed by Relaxation method. The number of iterations performed is 100 with the relaxation parameter set at 0.5. Compare this with figure (8).

RC FILTER, $RC=1$, $C=.01$

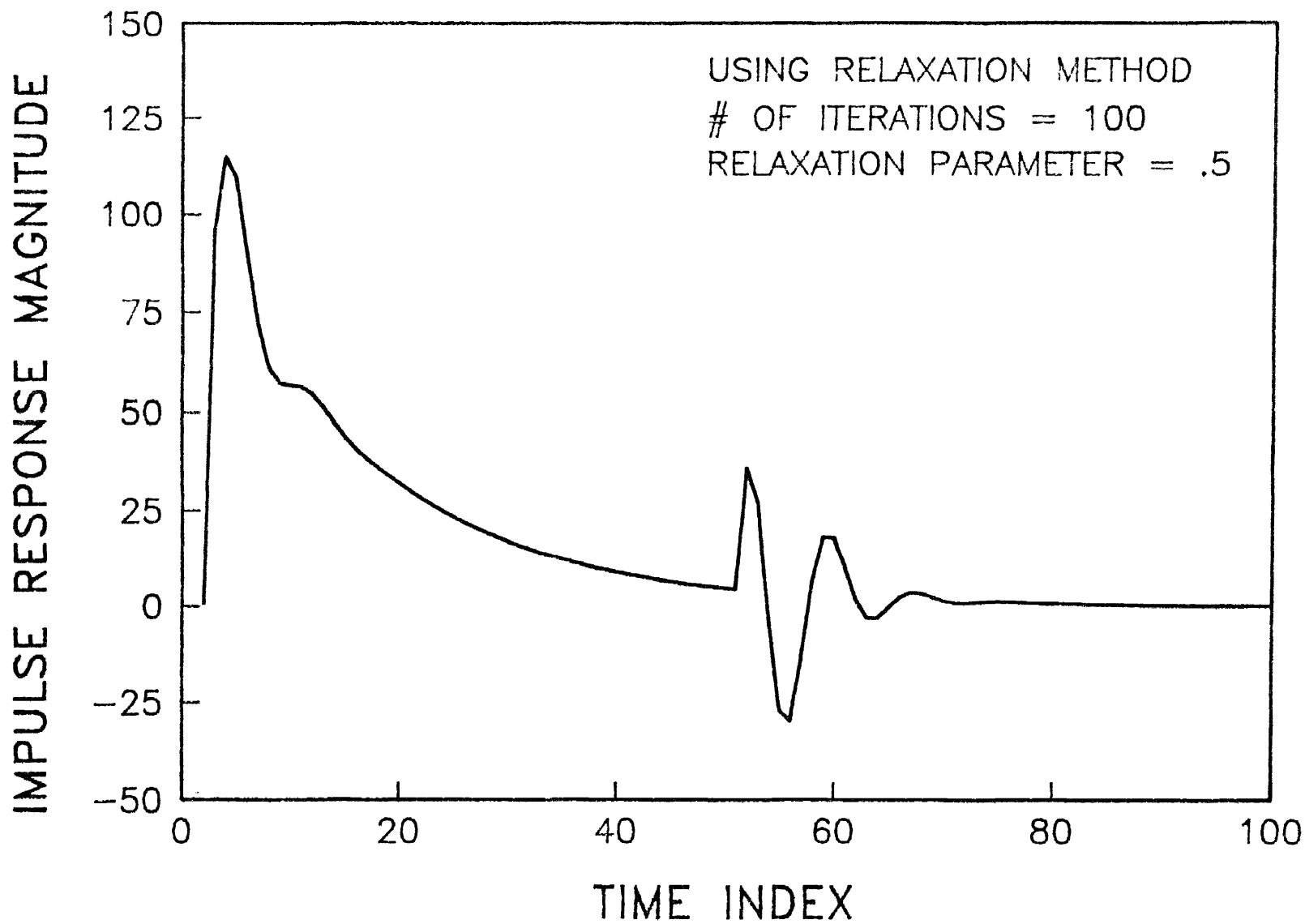


Fig. 8

FIGURE 9

Impulse response function (IRF) computed by the relaxation method with $k = 25$ and the relaxation parameter set at 0.1. Note that the IRF is sketched only up to $t = T/2$ for the purpose of enhancing the effects of the relaxation parameter.

RC NETWORK, $RC=1$, $C=.01$

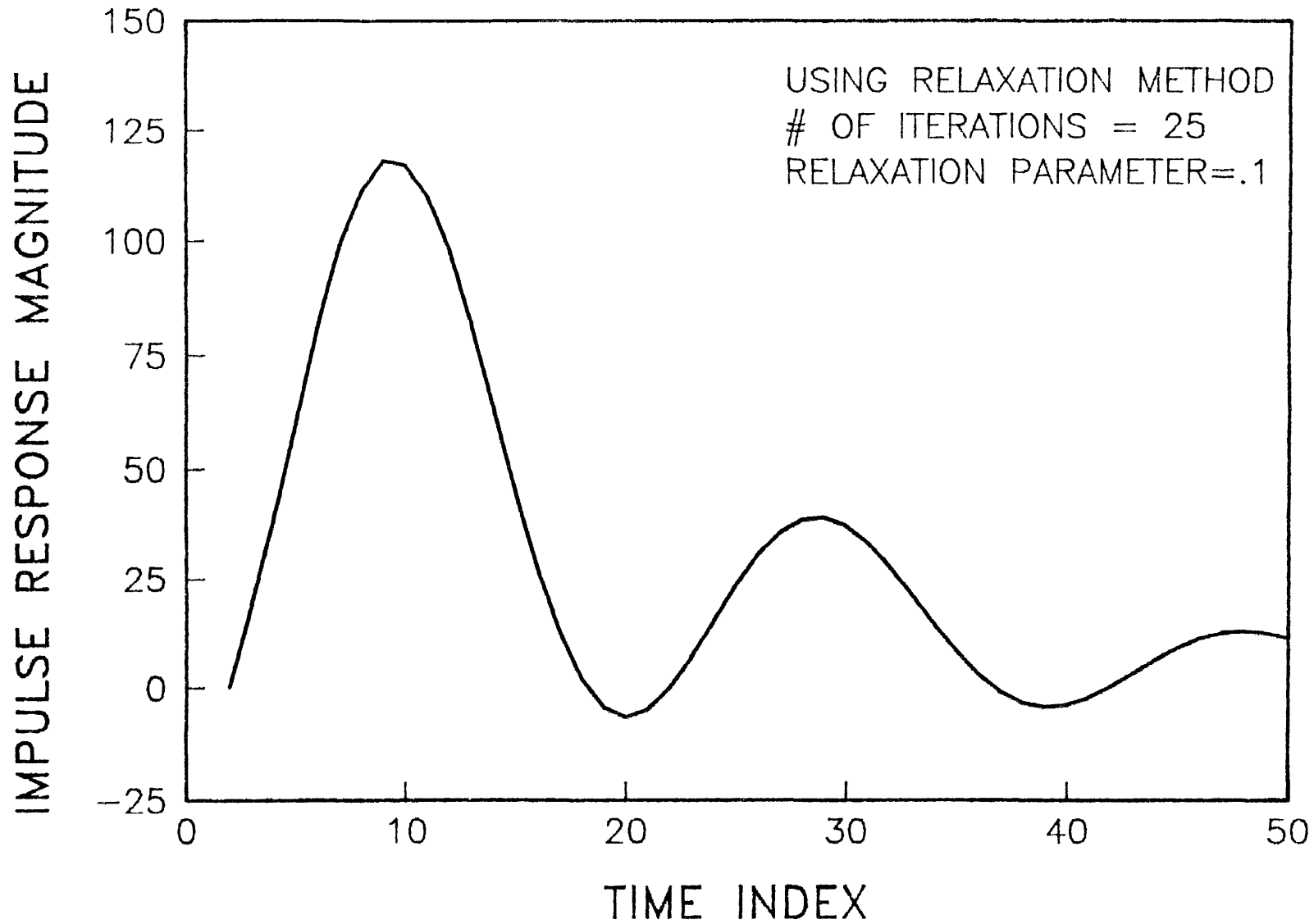


Fig. 9

FIGURE 10

Impulse response function(IRF) computed by the relaxation method with $k = 25$ and the relaxation parameter set at 0.5. Compare the results with those of figure(9).

RC FILTER $RC=1$, $C=.01$

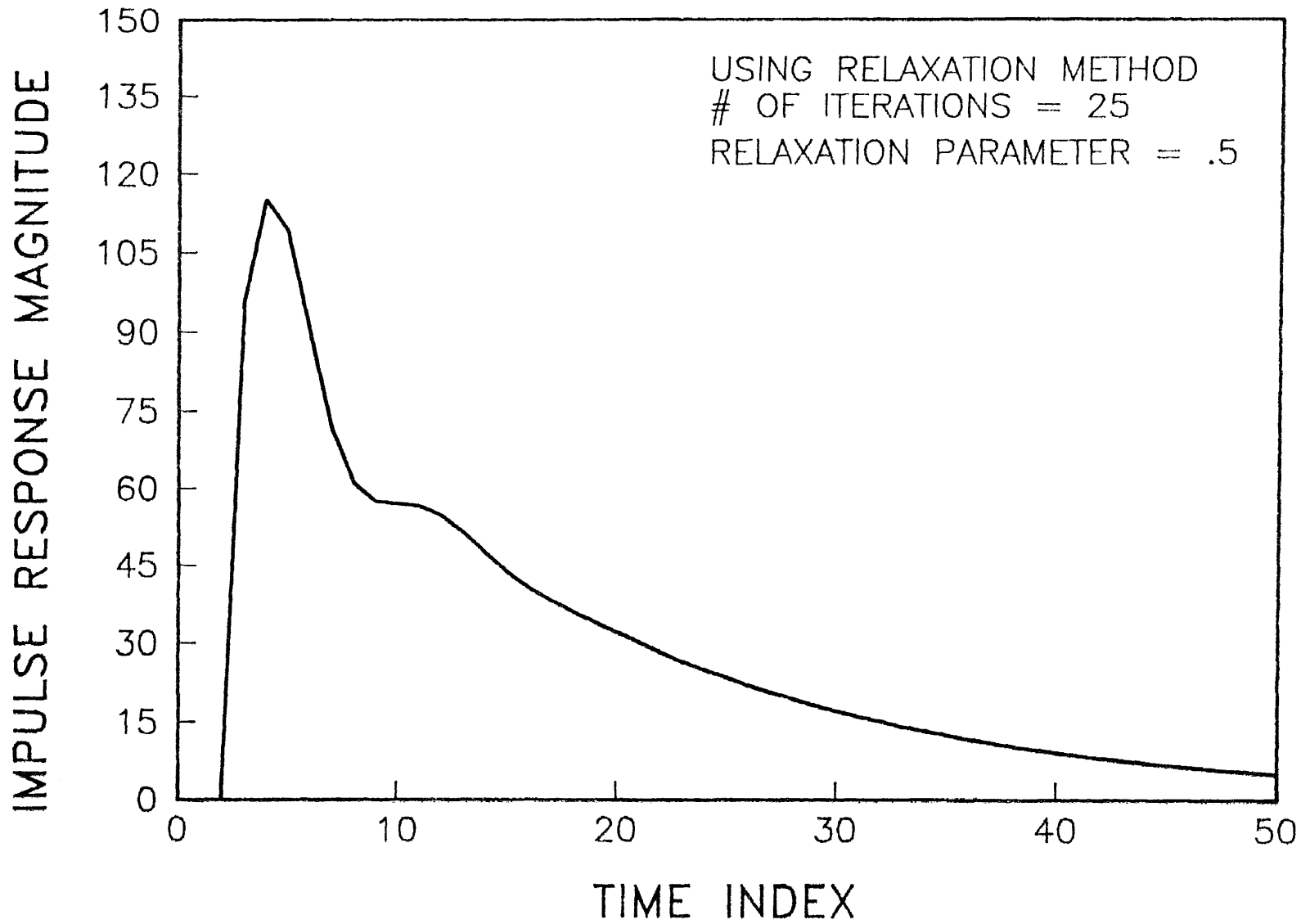


Fig. 10

FIGURE 11

Impulse response function(IRF) of the RC network computed by the relaxation method. $k = 25$, Relaxation parameter = 0.5. The start point is chosen $\text{att} = 2$. Note that the IRF is sketched only up to $t = T/2$ for the purpose of enhancing the effect of the start point.

RC NETWORK, $RC=1$, $C=.01$

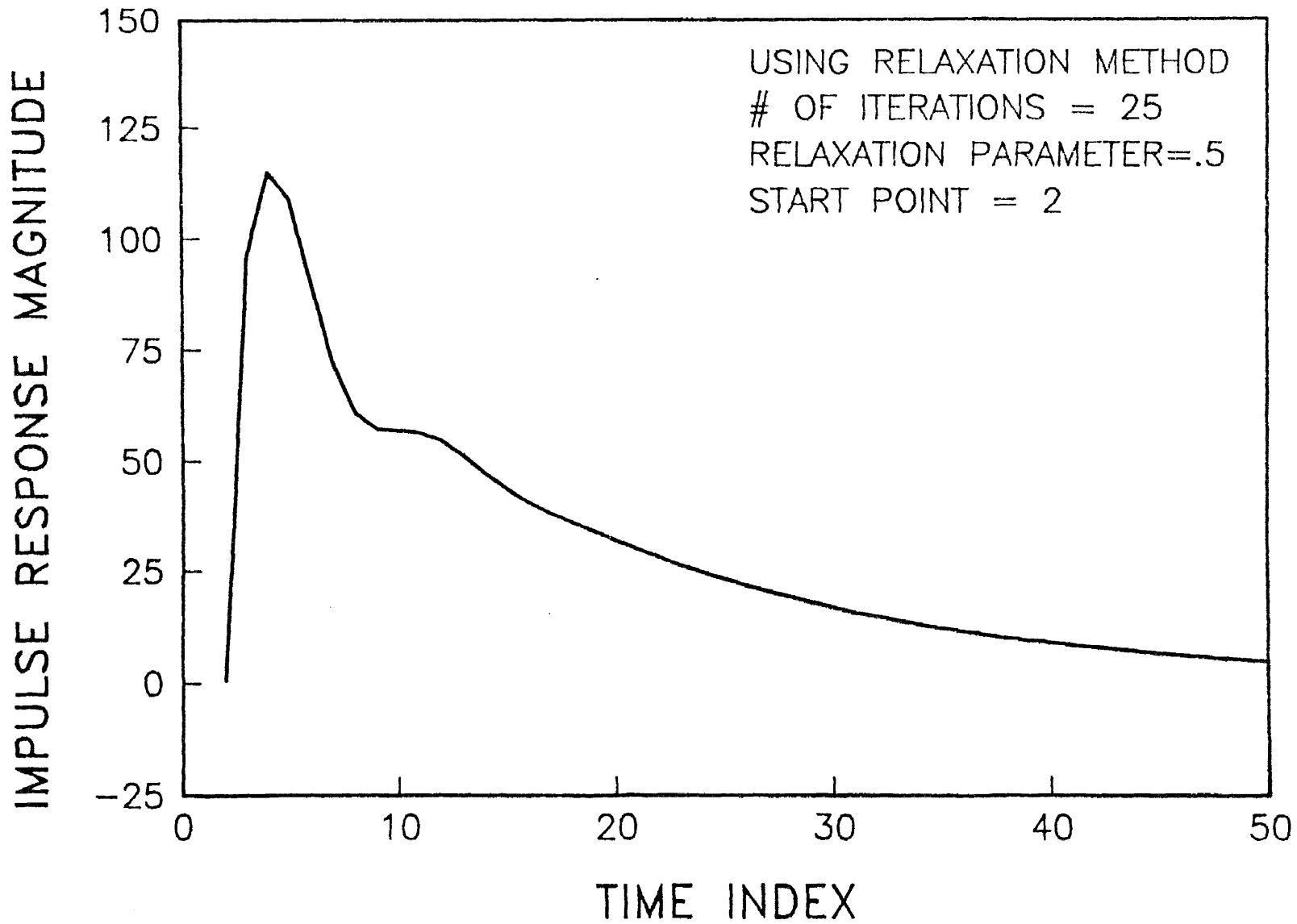


Fig. 11

FIGURE 12

Impulse response function (IRF) of the RC network computed by the relaxation method. $k = 25$, Relaxation parameter = 0.5 and start point, $t = 4$. Compare results with those of figure (11).

RC NETWORK, $RC=1$, $C=.01$

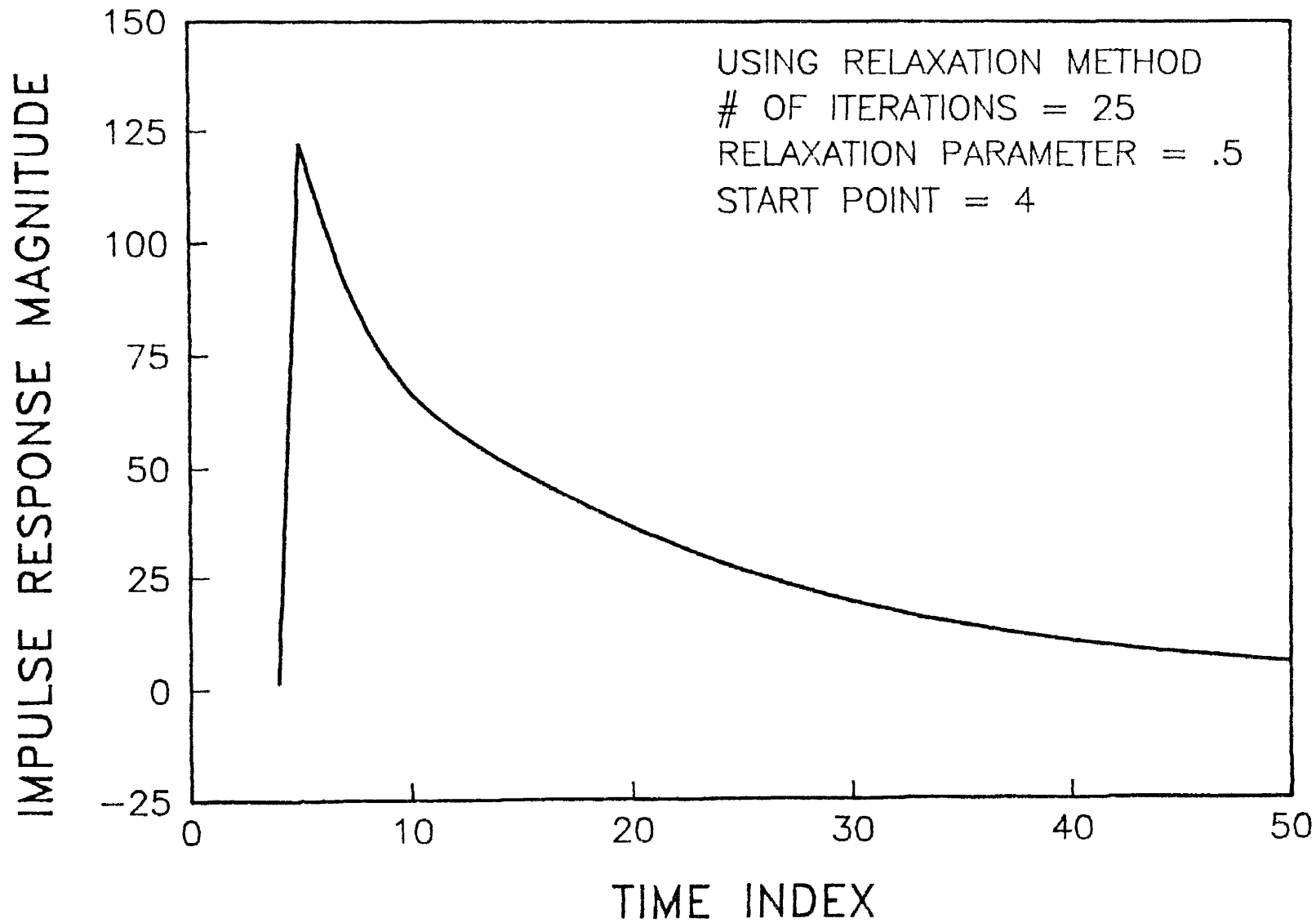


Fig. 12

FIGURE 13

Impulse response function of the RC Filter network using a modified relaxation procedure. With $t = 2$, the IRF shows oscillations with increasing amplitudes as t is increased.

RC NETWORK, RC=1, C=.01, DC=0, N=101

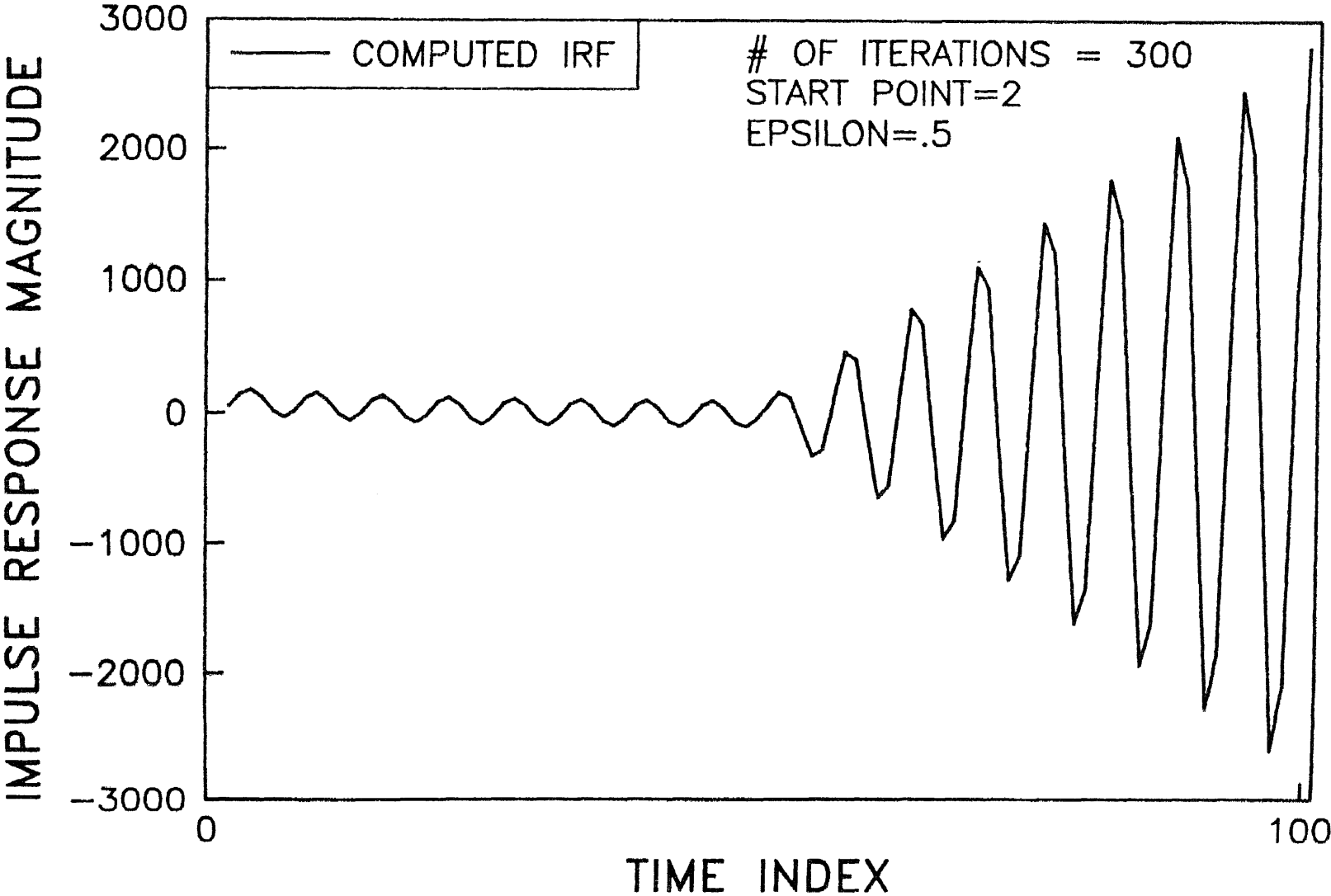


Fig. 13

FIGURE 14

Impulse response function of the RC network using the modified procedure with $t = 3$, Epsilon = 0.5 and $k = 201$.

RC NETWORK, $RC=1$, $C=.01$, $DC=0$, $N=101$

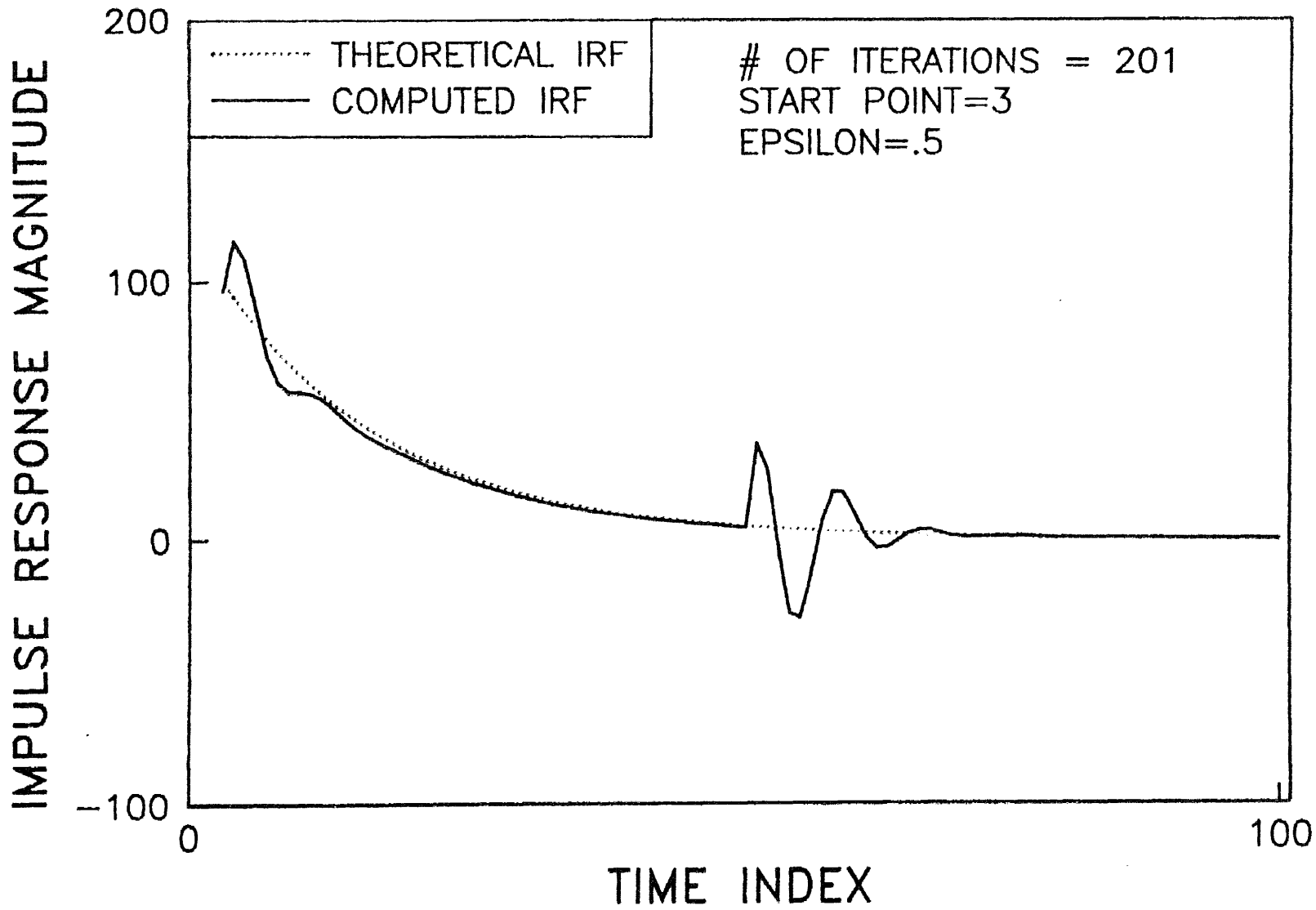


Fig. 14

FIGURE 15

Impulse response function of the RC network using the modified procedure with $t = 4$, $\text{Epsilon} = 0.5$ and $k = 201$.

RC NETWORK, $RC=1$, $C=.01$, $DC=0$, $N=101$

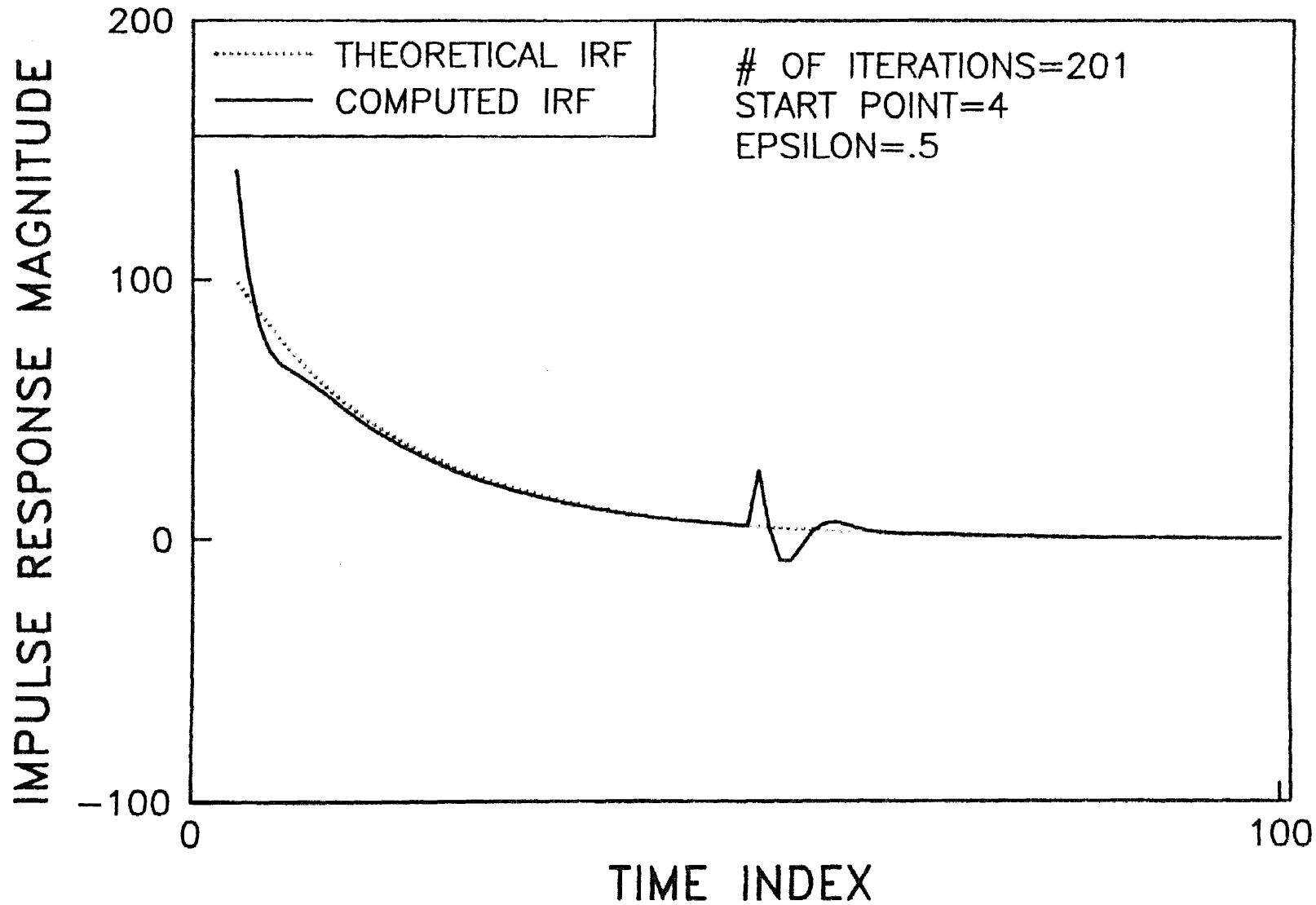


Fig. 15

FIGURE 16

Impulse response function of the RC network using the modified method with $t = 5$, Epsilon = 0.5 and $k = 201$.

RC NETWORK, $RC=1$, $C=.01$, $DC=0$, $N=101$

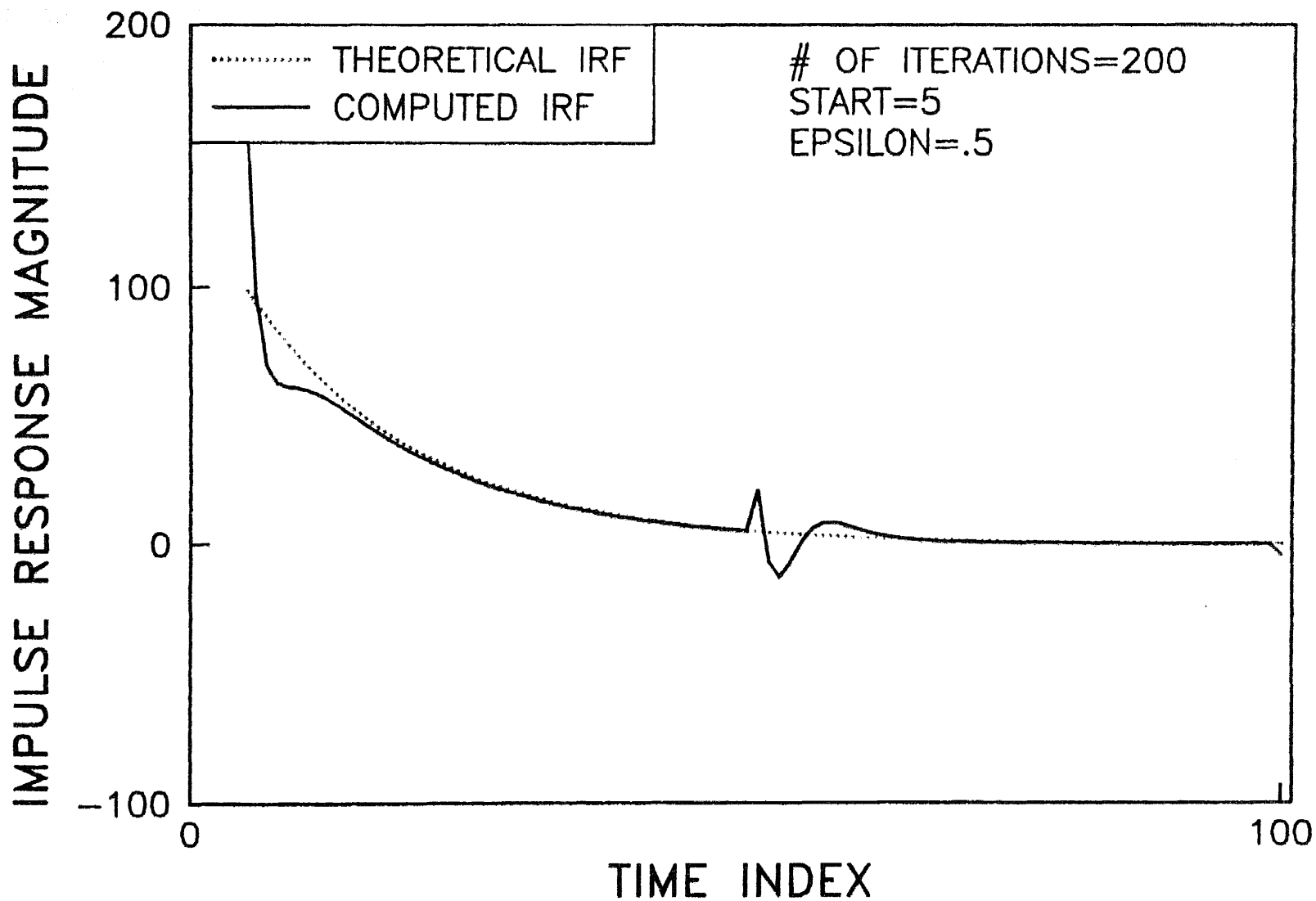


Fig. 16

FIGURE 17

Impulse response function of the RC network by the modified method method computed from experimentally generated data. $R = 13k$ ohms, $C = 20$ Farads Epsilon = .5 $k = 200$ and start point = 5. Compare with the results of figure(4).

RC NETWORK, R=13 KOHMS, C=20 MICROFARADS

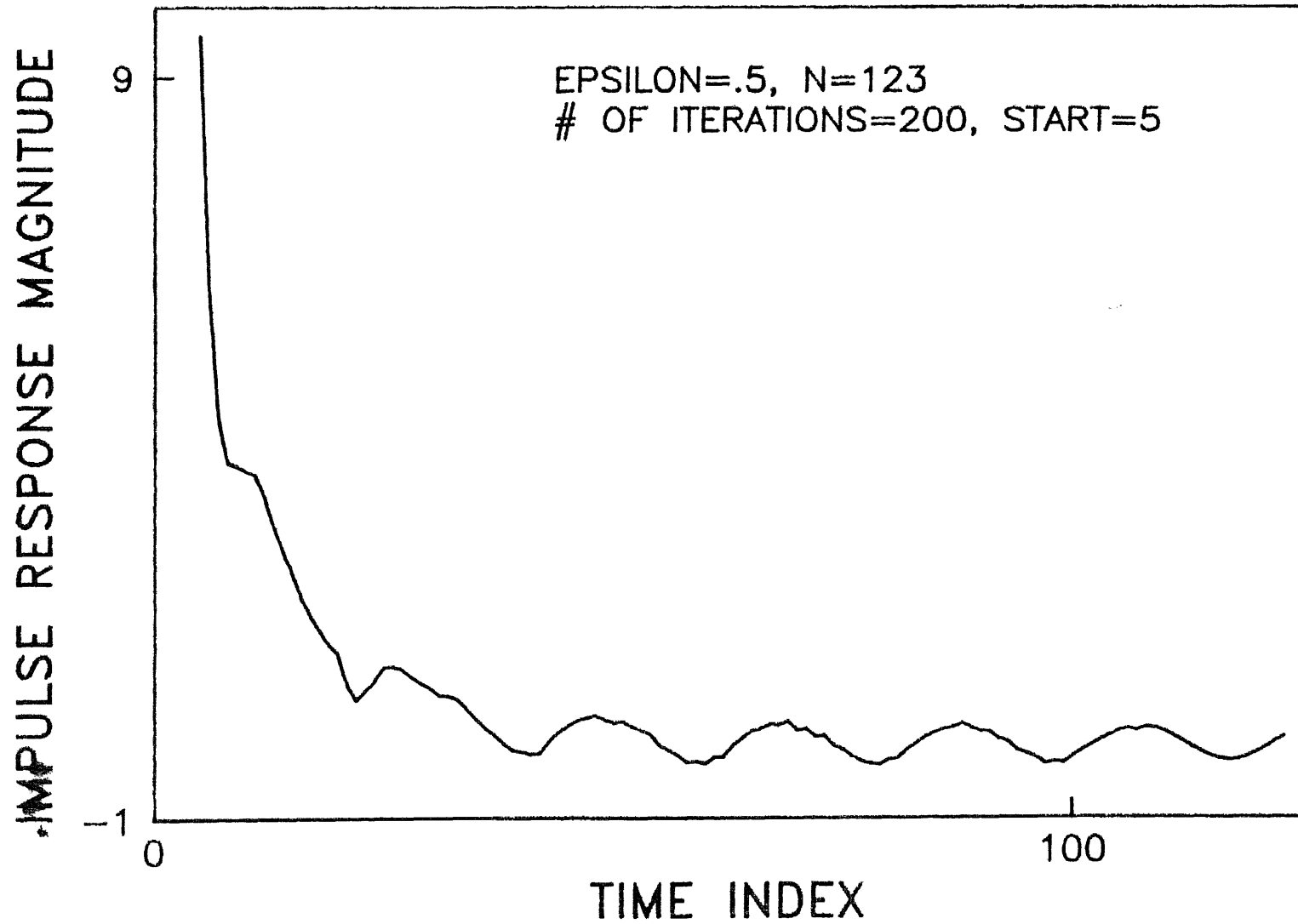


Fig. 17

FIGURE 18

Aortic pressure waveform obtained from a 3-element Windkessel model. Model parameters are given in the text.

WINDKESSEL MODEL — PRESSURE

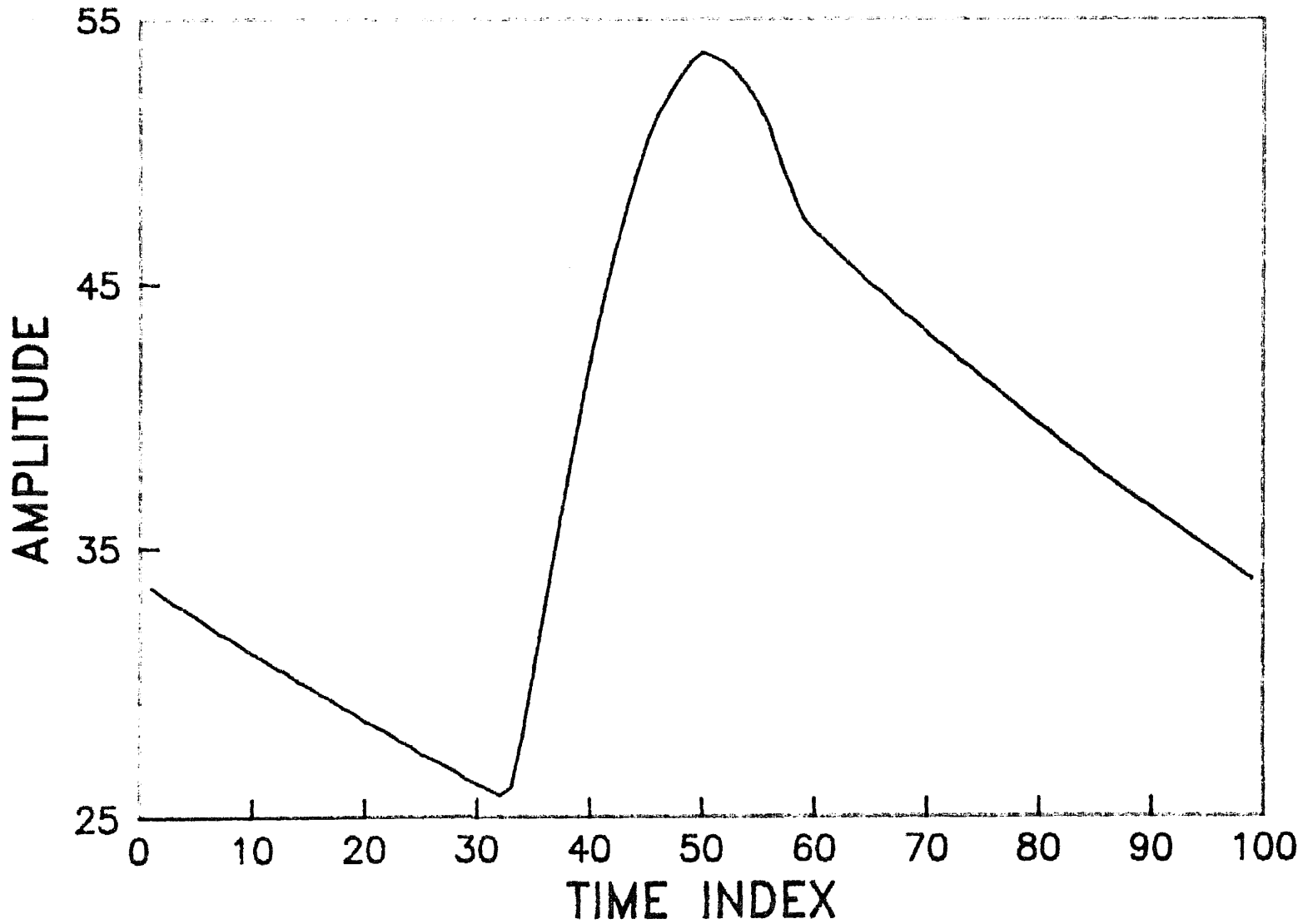


Fig. 18

FIGURE 19

Aortic Flow waveform obtained from a 3-element Windkessel model. Model parameters are given in the text.

WINDKESSEL MODEL — AORTIC FLOW

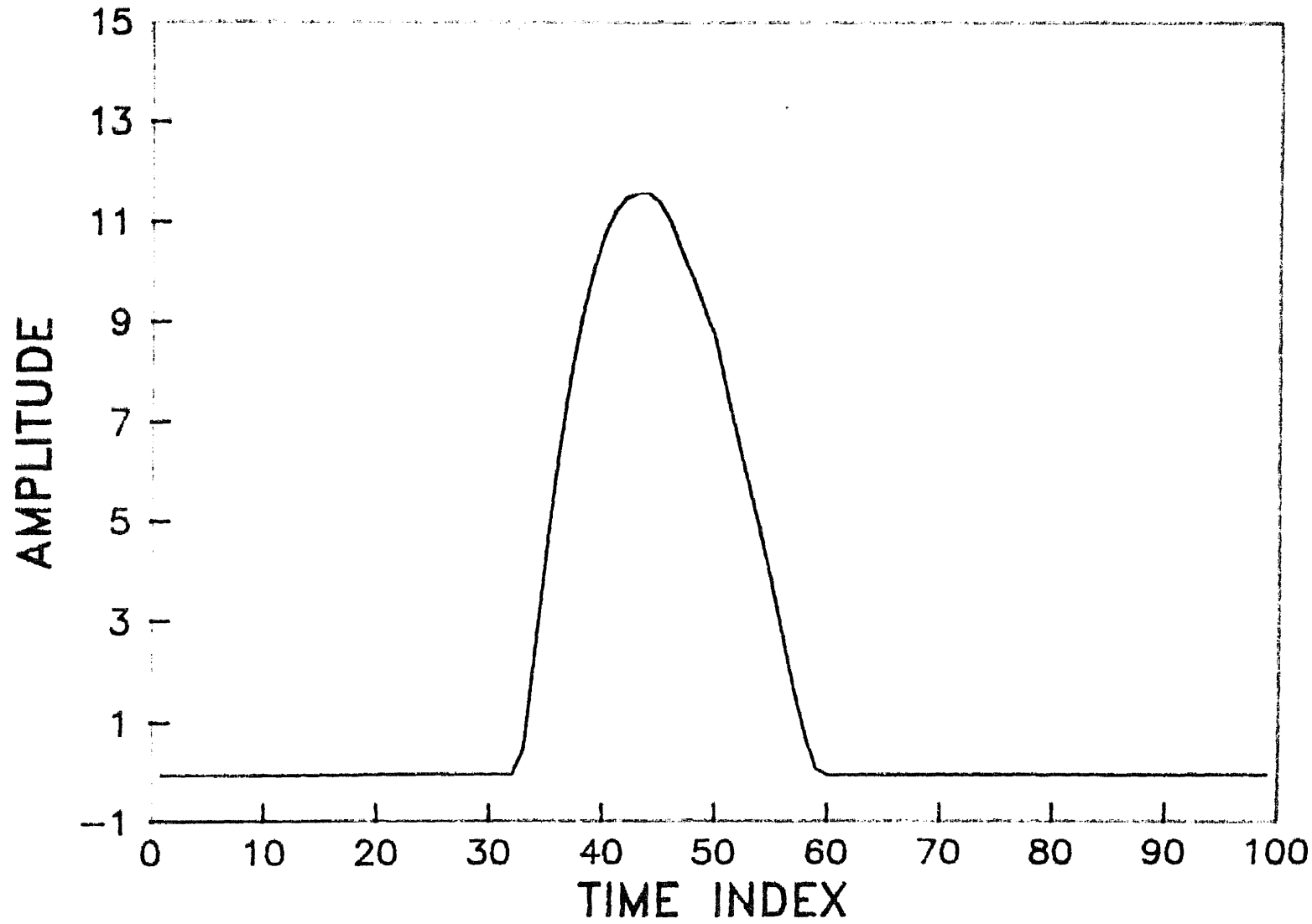


Fig. 19

FIGURE 20

Impulse Response Function of the Windkessel model computed by the direct method. The time index corresponds to a sample interval of 0.01 seconds

WINDKESSEL MODEL

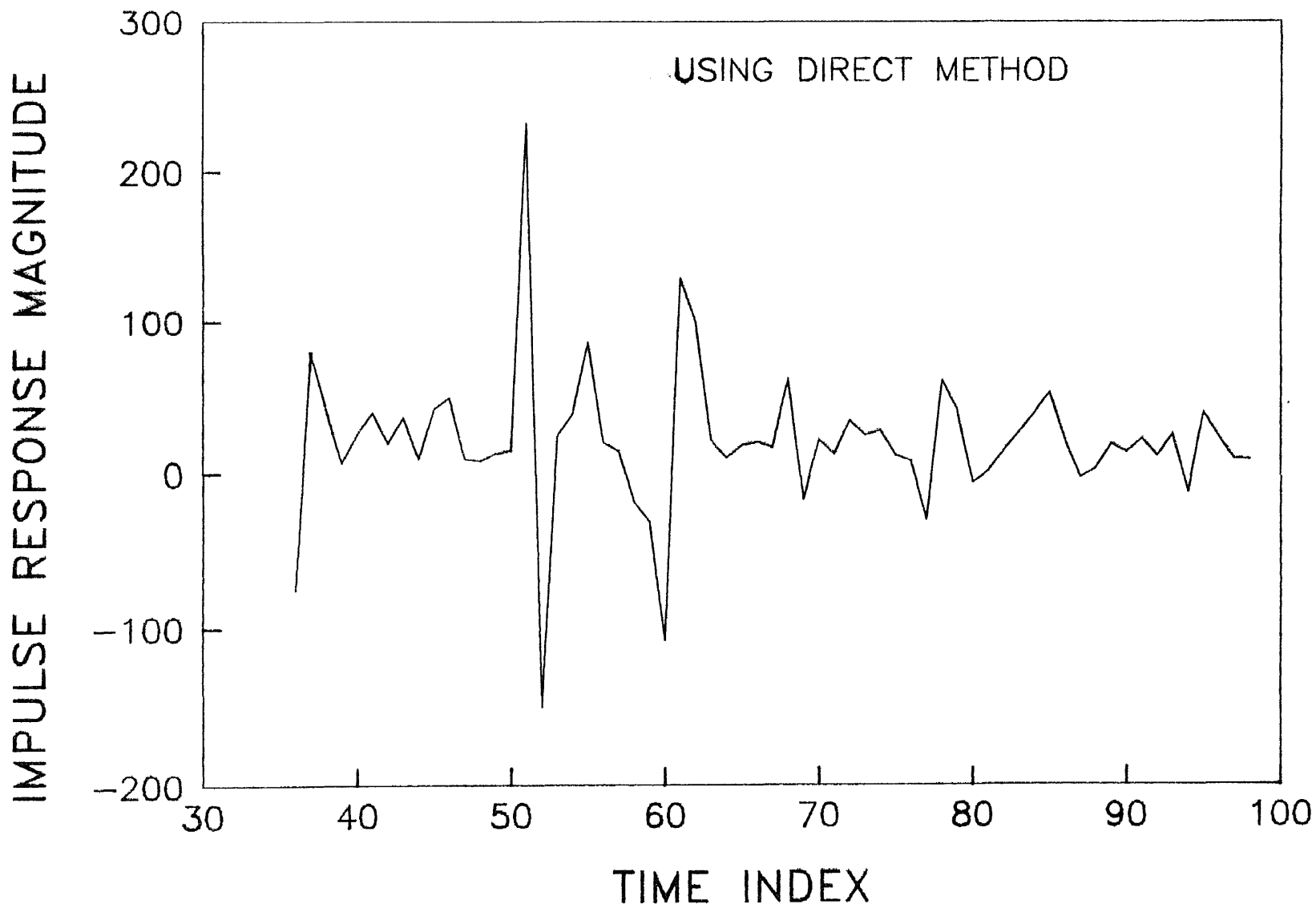


Fig. 20

FIGURE 21

Impulse Response Function of the Windkessel model computed by the modified relaxation method. Start point for deconvolution is set at $t = 34$ and $\text{Epsilon} = 0.5$.

WINDKESSEL MODEL

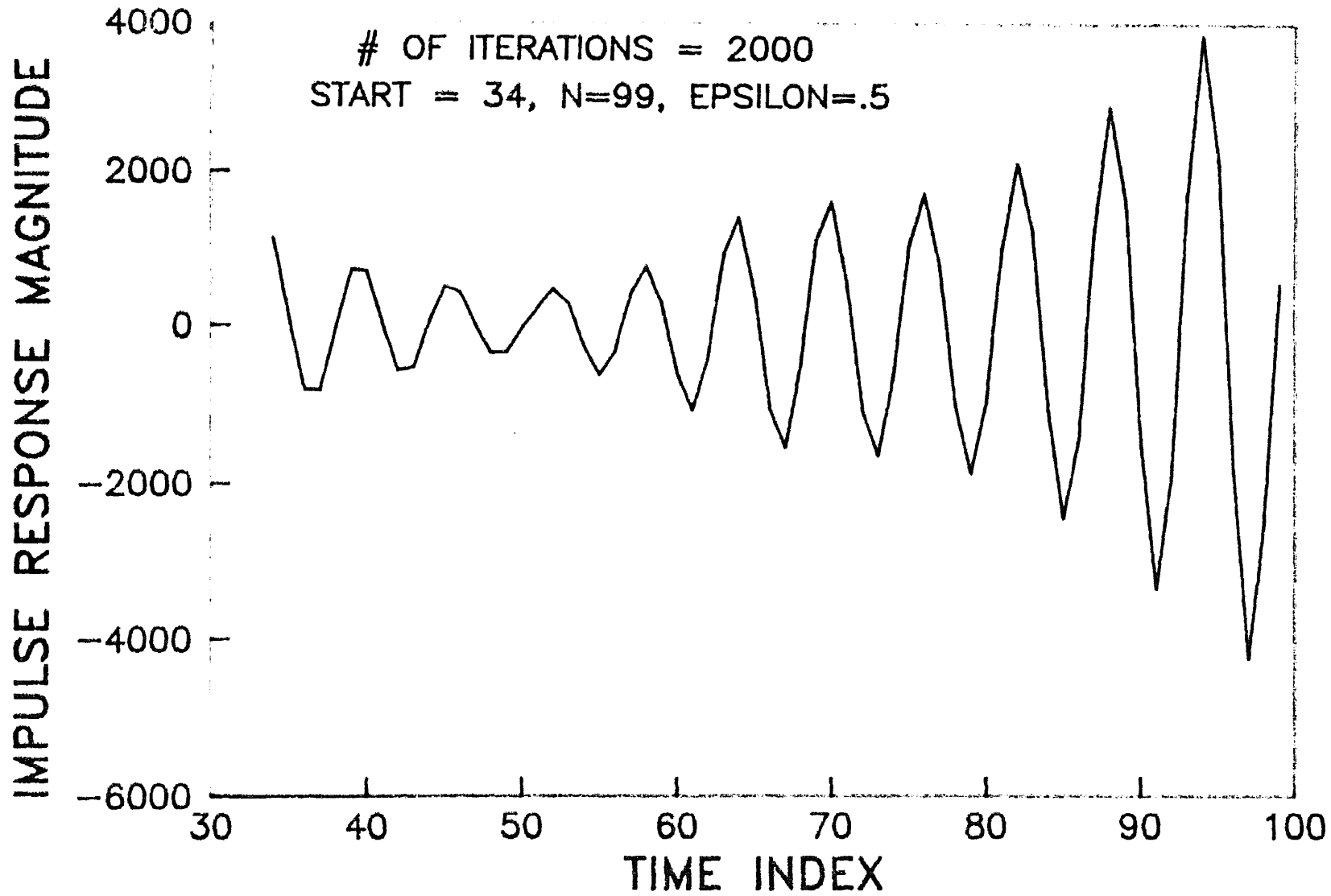


Fig. 21

FIGURE 22

Impulse Response Function of the Windkessel model computed by the modified relaxation method. Start point for deconvolution was set at $t = 34$ and the rest of the parameters are the same as in figure(20). Note the effect of start point between figure(21) and figure(22).

WINDKESSEL MODEL

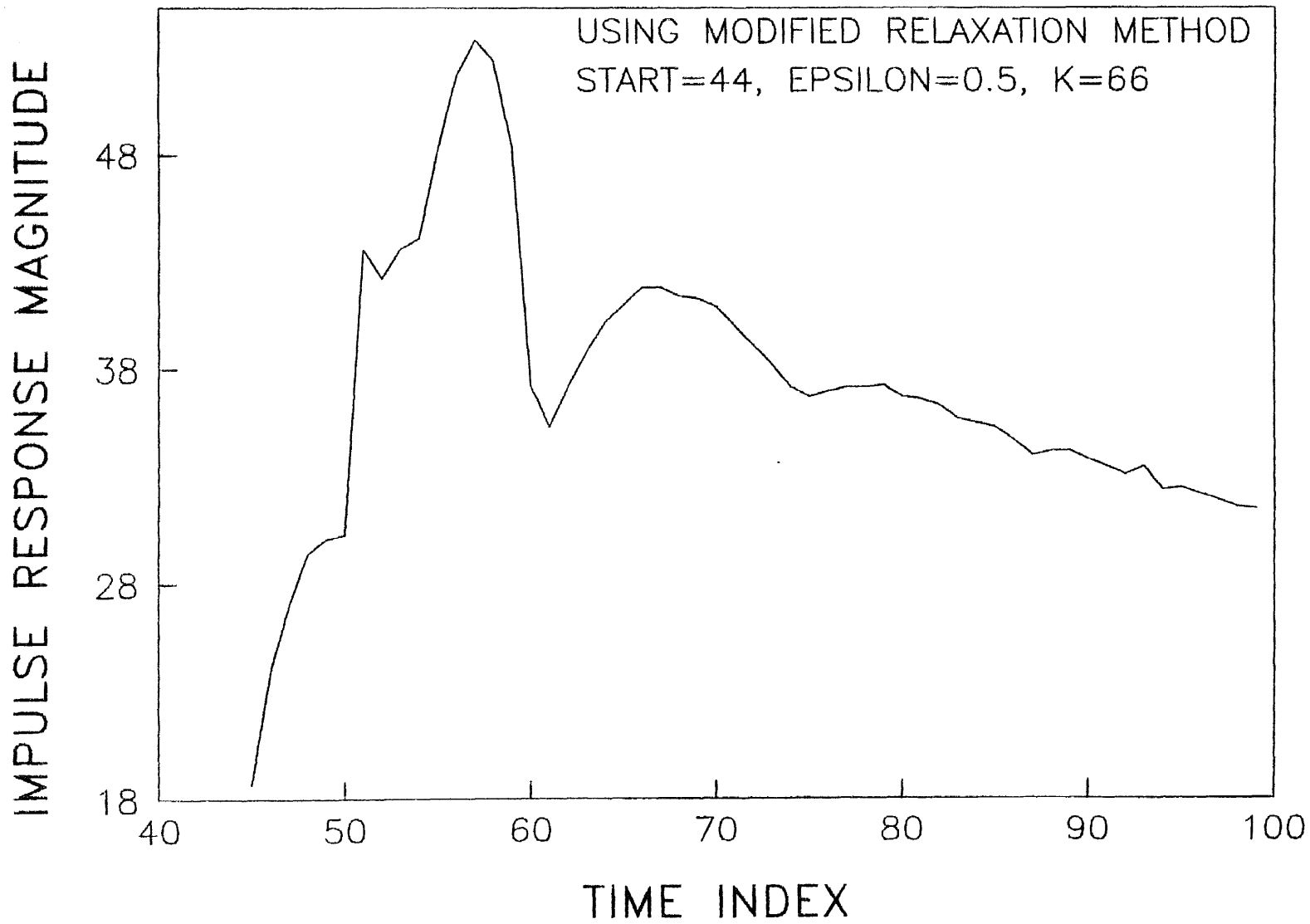


Fig. 22